

# Abundances, Ionization States, Temperatures, and FIP in Solar Energetic Particles

Donald V. Reames

IPST, University of Maryland, College Park, MD, USA

**Abstract** The relative abundances of chemical elements and isotopes have been our most effective tool in identifying and understanding the physical processes that control populations of energetic particles. The early surprise in solar energetic particles (SEPs) was 1000-fold enhancements in  ${}^3\text{He}/{}^4\text{He}$  from resonant wave-particle interactions in the small “impulsive” SEP events that emit electron beams that produce type III radio bursts. Further studies found enhancements in Fe/O, then extreme enhancements in element abundances that increase with mass-to-charge ratio  $A/Q$ , rising by a factor of 1000 from He to Pb arising in magnetic reconnection regions on open field lines in solar jets. In contrast, in the largest SEP events, the “gradual” events, acceleration occurs at shock waves driven out from the Sun by fast, wide coronal mass ejections (CMEs). Averaging many events provides a measure of solar coronal abundances, but  $A/Q$ -dependent scattering during transport causes variations with time; thus if Fe scatters less than O, Fe/O is enhanced early and depleted later. To complicate matters, shock waves often reaccelerate impulsive suprathermal ions left over or trapped above active regions that have spawned many impulsive events. Direct measurements of ionization states  $Q$  show coronal temperatures of 1 – 2 MK for most gradual events, but impulsive events often show stripping by matter traversal after acceleration. Direct measurements of  $Q$  are difficult and often unavailable. Since both impulsive and gradual SEP events have abundance enhancements that vary as powers of  $A/Q$ , we can use abundances to deduce the probable  $Q$ -values and the source plasma temperatures during acceleration,  $\approx 3$  MK for impulsive SEPs. This new technique also allows multiple spacecraft to measure temperature variations across the face of a shock wave, measurements otherwise unavailable. Comparing coronal abundances from SEPs and from the slow solar wind, remaining differences are for the elements C, P, and S. We propose that these elements, with intermediate values of first ionization potential (FIP), act like high-FIP neutral atoms in cool sunspots beneath active regions where SEPs are accelerated, but behave like low-FIP ions in the warmer photosphere that contributes to the slow solar wind, ions being more readily swept into the corona than neutral atoms. In addition, shock waves can accelerate ions from closed coronal loops (with footpoints in sunspots) that easily escape as SEPs, while the solar wind must emerge on open fields.

**Keywords** Solar energetic particles · Shock waves · Coronal mass ejections · Solar flares · Solar system abundances · Solar wind

## 1 Introduction

Relative abundances of the chemical elements and isotopes show striking variety in the populations of energetic particles we see, and they have given us the leverage to understand the physics of the particle origin. Examples include: (i) Dominance of energetic S and O in the Jovian magnetosphere points to sulfurous gasses emitted from volcanoes on the moon Io. (ii) Nearly pure H in the inner radiation belt of Earth results from the decay of neutrons produced in interactions of galactic cosmic rays (GCRs) with atoms in the Earth's atmosphere. (iii) The abundance of the rare elements Li, Be, and B in the GCRs themselves attest to the GCR interaction with interstellar H during their  $\sim 10^7$  yr sojourn in the Galaxy. (iv) Anomalous cosmic rays (ACRs) contain only elements with high first ionization potential (FIP) that are neutral atoms in interstellar space so they easily penetrate the magnetic fields of the heliosphere to approach the Sun, where they are photo-ionized, picked up by the solar wind, and preferentially accelerated in the outer heliosphere, a complex journey. Where would we be without abundances? They give essential information and are signatures that identify populations of particles.

Probably the most unusual abundance pattern we know is in the little “impulsive” events of solar energetic particles (SEPs), the  $^3\text{He}$ -rich events. The abundance of the rare isotope  $^3\text{He}$  can be enhanced by factors up to  $10^4$  in these events. In a few events  $^3\text{He}$  exceeds H. Otherwise-rare heavy elements are also enhanced when compared with the corresponding abundances from the solar corona. First we found Fe/O enhanced a factor of  $\sim 10$ , and later we found the element abundances rising as a power law in their mass-to-charge ratio  $A/Q$  by a factor of  $\sim 1000$  right across the periodic table from He to Pb. The impulsive SEP events have been associated with magnetic reconnection near the Sun in solar plasma jets that produce narrow, but slow, coronal mass ejections (CMEs) and also accelerate the beams of electrons that produce type III radio bursts. It may be those electron beams that produce copious plasma waves at the gyrofrequency of  $^3\text{He}$  that are resonantly absorbed to selectively enhance energetic  $^3\text{He}$ . These events carry their characteristic abundance signature, like a beacon, wherever they appear. Meanwhile, we can use the strong power-law dependence on  $A/Q$ , with its associated pattern of charge states of the elements, to deduce an electron temperature of about 3 MK (1 MK  $\equiv 10^6$  K) at the source of the ion acceleration. Abundances of impulsive SEP events are presented in Section 2.1.

By way of contrast, the average abundances of elements in the large “gradual” SEP events, like those in the solar wind, provide a measure of element abundances in the solar corona. Coronal abundances differ from those in the solar photosphere as a bilevel function of the first ionization potential (FIP) of the ion. Elements with low FIP ( $< 10$  eV) such as Mg, Si, and Fe, are ionized in the photosphere and are more easily swept up into the corona than high-FIP elements, like He, O, and Ne, that begin as neutral atoms in the photosphere. Thus the low-FIP elements are a factor of  $\sim 3$  more abundant. All atoms become highly ionized at the  $\sim 1$  MK temperature of the corona where they are available to be accelerated by shock waves driven out from the Sun by fast, wide CMEs to produce gradual SEP events. Scattering of SEPs streaming out from the source depends upon particle rigidity, or upon  $A/Q$  at a given velocity, so that Fe scatters less than O, for example. This creates regions of enhanced Fe/O where Fe has forged ahead and regions

of depleted Fe/O behind. This time dependence is converted into longitude dependence by solar rotation. While these regions may average to give the coronal abundance, the individual regions provide a pattern of  $Q$ -dependence that again allows us to determine a source plasma temperature, usually  $\sim 1 - 2$  MK where about half the electrons have been removed from Fe. In some active regions, shock waves also reaccelerate suprathermal ions left over from previous *impulsive* SEP events. Then a component of the  $^3\text{He}$ -rich, Fe-rich, 3 MK plasma shines through. Abundances in gradual events are discussed in Section 2.2

Measurements of ionization states of heavier ions such as Fe can tell us the typical plasma temperature from which they came and thus help identify their origin. Such measurements have been made directly in instruments, and by using the geomagnetic field. In either case, deflection of particles of a given velocity by electric or magnetic fields in an instrument depends upon their mass-to-charge ratio  $A/Q$ . Unfortunately, the instruments are complex, are limited to low energy, and are rarely available, while the geomagnetic measurements are local and are not possible throughout in the heliosphere.

However, the physical processes of SEP acceleration and transport *themselves* involve electric and magnetic fields, so the relative enhancement and suppression of different species at a given velocity *also* depends upon  $A/Q$ . Conveniently for us, element abundances are frequently altered as powers of  $A/Q$ . *Why not use the  $A/Q$ -dependent element abundances nature has already provided to determine  $Q$ -values and electron temperatures of the source plasma? Perhaps the electric and magnetic fields near the particle's source can analyze the ions for us just as well as the field of the Earth or those in instruments.* As a bonus, the ionization states deduced are often those at the original source, unaltered by later stripping in transit. Unfortunately the new technique does not measure *distributions* of  $Q$  and temperature, so direct measurements are still important, but the extended coverage of mean values of  $Q$  and  $T$  for many more SEP events is a great benefit. Ionization states, especially these new techniques, are discussed in Section 3 and variations in the source abundances of SEPs, especially He, in Section 4.

Thus we review details of measurements of SEP abundance and charge states and the physical processes those measurements have helped us understand. It is no surprise that abundances have already contributed significantly to our understanding of SEPs. This gives us a basis to describe the new method of using power-law abundance enhancements to determine source plasma temperatures and the early findings from that technique. We then turn to the “FIP-effect” and the SEP view of the corona, as compared with that of the solar wind. *This comparison results in a surprising new suggestion of the unique effect of cool sunspots on abundances of C, P, and S in SEPs in Section 5.* There can also be differences in the regions where SEPs and the solar wind can be selected; *shock waves can sample ions from closed, but weak, high coronal loops to generate SEPs that easily escape, but the solar wind must come only from open field lines.*

In Section 6 we return to ionization states and temperatures and discuss early results in mapping them in space and time across an accelerating shock wave, followed by a general discussion of relevant consequences (Section 7) and summary (Section 8).

## 2 SEP Abundances

### 2.1 Impulsive SEP events

$^3\text{He}$ -rich events were first observed by Hsieh and Simpson (1970). To a community familiar with nuclear fragmentation of GCRs they were first thought to be produced by nuclear reactions in solar flares, but there was no evidence of  $^2\text{H}$ ,  $^3\text{H}$ , or other reaction secondaries. Then Serlemitsos and Balasubrahmanyam (1975) found  $^3\text{He}/^4\text{He} = 1.52 \pm 0.10$ , compared with  $(4.08 \pm 0.25) \times 10^{-4}$  in the solar wind (Gloeckler and Geiss 1998), but they also found  $^3\text{He}/^2\text{H} > 300$ . How could so much  $^3\text{He}$  be produced in nuclear reactions with no  $^2\text{H}$  or  $^3\text{H}$ ? Yet, there is certainly evidence of nuclear reactions in the corona in flares from the neutrons (Evenson et al. 1983, 1990) and  $\gamma$ -ray lines (e.g. Ramaty and Murphy 1987; Kozlovsky, Murphy, and Ramaty 2002) we see from the footpoints of magnetic loops during flares. However, isotopes of Li, Be, and B, also expected from the  $\gamma$ -ray lines, have never been observed in SEPs in space. Limits on Be/O or B/O in large SEP events are  $< 2 \times 10^{-4}$  (e.g. McGuire, von Rosenvinge, and McDonald 1979; Cook, Stone, and Vogt 1984). Neutrals from nuclear reactions escape, but charged particles cannot escape the closed magnetic loops of solar flares.

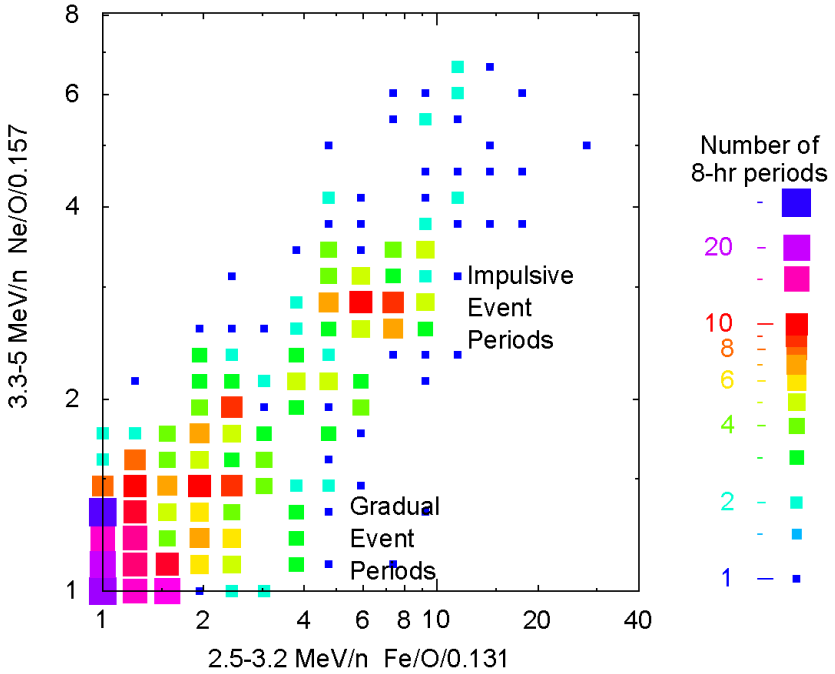
Thus the ions we see in space are accelerated in reconnection events on the open magnetic fields of solar jets (e.g. Kahler, Reames, and Sheeley 2001; Reames 2002) rather than those on the closed loops of flares. Furthermore, the huge enhancement of  $^3\text{He}$  is not produced in nuclear reactions at all, but by preferential acceleration in resonant wave-particle interactions at the gyrofrequency of  $^3\text{He}$ . A variety of preferential heating mechanisms were suggested (e.g. Fisk 1978) but acceleration remained elusive. A spectrum of waves would be absorbed at the gyrofrequencies of the most abundant species in the plasma,  $^1\text{H}$  and  $^4\text{He}$ , but the much rarer  $^3\text{He}$  could absorb considerable energy at its gyrofrequency, which lies alone between those of the two most abundant species, without significantly damping the waves there.

Early observations found non-relativistic electron events in space (e.g. Lin 1974) that were associated with small impulsive X-ray events at the Sun and with the production of metric type III radio bursts. Lin thought many of these to be “pure” electron events, lacking observable protons or other ions. However,  $^3\text{He}$ -rich events were subsequently associated with these electron events (Reames, von Rosenvinge, and Lin 1985) and directly with both metric and kilometric type III radio bursts (Reames and Stone 1986). Later, it was suggested that these streaming electrons produced electromagnetic ion-cyclotron waves that resonated with mirroring  $^3\text{He}$  ions to produce the striking enhancements in  $^3\text{He}$ -rich SEP events (Temerin and Roth 1992; Roth and Temerin 1997). More recently, Liu, Petrosian, and Mason (2006) have been able to fit the complex spectra of  $^3\text{He}$  and  $^4\text{He}$  (Mason 2007).

With improving measurements, it was found that heavy-ion abundances, such as Fe/O, were also enhanced in  $^3\text{He}$ -rich events (e.g. Mason et al. 1986; Reames, Meyer, and von Rosenvinge 1994) and Fe/O became a more reliable indicator of impulsive events than  $^3\text{He}/^4\text{He}$ , since the latter varies strongly with energy while Fe/O is better behaved (Mason 2007). In fact, with modern data, when we simply look at Ne/O vs. Fe/O in all 8-hr periods during 19 years, we find the distribution in Figure 1. Data in this figure are unbiased with respect to time or event selection, although, clearly, individual gradual events occupy many more time periods, and many small impulsive events with too few

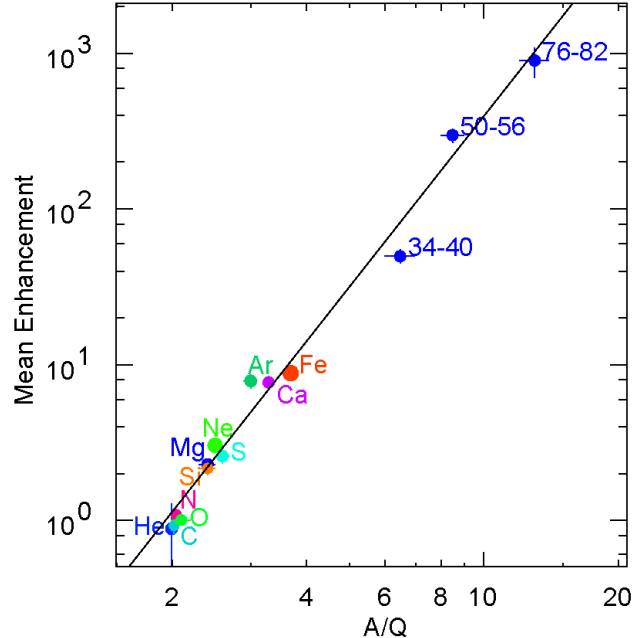
ions are overlooked. This bimodal (Reames 1988) abundance distribution helps resolve the populations of impulsive and gradual SEP events.

**Fig. 1** Values of enhancements of Ne/O vs. Fe/O near 3 MeV  $\text{amu}^{-1}$  are binned for all 8-hr intervals during 19 years which have errors of 20% or less. The cluster of periods near the origin at (1, 1) represents gradual SEP event periods, that determine the normalization factors. The peak near (7, 3) is from the impulsive SEP events.



Eventually observations were extended to the rest of the periodic table above Fe (Reames 2000; Mason et al. 2004; Reames and Ng 2004), although *not* with single-element resolution. The enhancement of these heavy ions, relative to their coronal abundance rises as a power of  $A/Q$ , with  $Q$ -values defined at a temperature of  $\sim 3$  MK, rising three orders of magnitude between He and Pb (Reames 2000; Mason et al. 2004; Reames and Ng 2004; Reames, Cliver, and Kahler 2014a) as seen in Figure 2.

**Fig. 2** The mean enhancements in the abundances of elements in impulsive SEP events, relative to reference “coronal” abundances defined in gradual SEP events, is shown as a function of  $A/Q$  of the element with  $Q$ -values defined at  $\sim 3$  MK. Elements are identified by name or by intervals if atomic number  $Z$ . For the least-squares fit line shown in the figure the enhancement varies as the  $3.64 \pm 0.15$  power of  $A/Q$  (Reames, Cliver, and Kahler 2014a).



The recent measurements (Reames, Cliver, and Kahler 2014a) strongly associate the impulsive events with slow, narrow CMEs supporting their origin in solar jets, originally suggested by Kahler, Reames, and Sheeley (2001, see also Reames 2002 and review of jets by Raouafi et al. 2016). The CMEs associated with impulsive SEP events rarely drive shock waves since they move along  $B$  at less than the Alfvén speed (Vrsnak and Cliver 2008), thus they lack radio type II bursts, and their mean width is  $75^\circ$  vs.  $>130^\circ$  for those associated with gradual SEP events. The association with jets is strengthened by the presence of beamed electrons and type III-burst association of impulsive SEP events, but the enhancement of the heavy elements as a function of  $A/Q$  appears in particle-in-cell simulations (e.g. Drake et al. 2009) to result directly during the collapse of islands of magnetic reconnection in the solar jets. Other properties of impulsive SEP events have been reviewed by Mason (2007) and by Reames (2017a).

## 2.2 Gradual SEP events

The first SEP events observed were sufficiently large for GeV protons to produce fragments from nuclear interactions in the Earth's atmosphere that were detectable at ground level (Forbush 1946). These ground-level enhancements (GLEs) revealed nothing whatever about the abundances of the elements in the impinging SEPs. Nevertheless, even in the earliest sounding rocket observations of C, N, and O (Fichtel and Guss 1961) and of Fe (Bertsch, Fichel, and Reames 1969) and later measurements in space (e.g. Teegarden, von Rosenvinge, and McDonald 1973), authors attempted comparisons with abundances of the solar corona. However, with increasing measurements of SEP abundances in space it was found that the abundances, averaged over many events, divided by the corresponding solar photospheric abundances (knowledge of which was also evolving) showed a difference of a factor of  $\sim 3$  in the levels of elements with low and high FIP (Webber 1975; Meyer 1985).  $^3\text{He}$ -rich events were explicitly excluded from this average by Meyer. The individual SEP events forming the average showed a “mass-bias” or a dependence on  $A/Q$  according to Meyer (1985).

With improving instruments, average abundances from gradual SEP events (Reames 1995, 2014) are a standard for comparison with the corona and solar wind (Mewaldt et al. 2002; Schmelz et al. 2012). Figure 3 shows a recent FIP plot of average element abundances in SEPs (Reames 2014, 2017a) divided by the corresponding photospheric abundances where the dominant element species are from Caffau et al. (2011) supplemented by other elements from Lodders, Palme, and Gail (2009). The difference in FIP levels arises because the high-FIP elements are neutral atoms in the photosphere while the low-FIP elements are ions. The ions are more easily convected up into the corona by the action of Alfvén waves, for example (e.g. Laming 2009, 2015).

A comparison of the FIP dependence using the alternative photospheric abundances of Asplund et al. (2009) is shown by Reames (2015). SEP He abundances from events with different source plasma temperatures are shown in Figure 3 and are discussed in Section 4.1. We will compare FIP plots for SEPs with that for the solar wind in Section 5. Whenever we talk about “enhancements” in this paper, we mean observed abundance ratios divided by these average SEP abundances, i.e. the SEP corona.

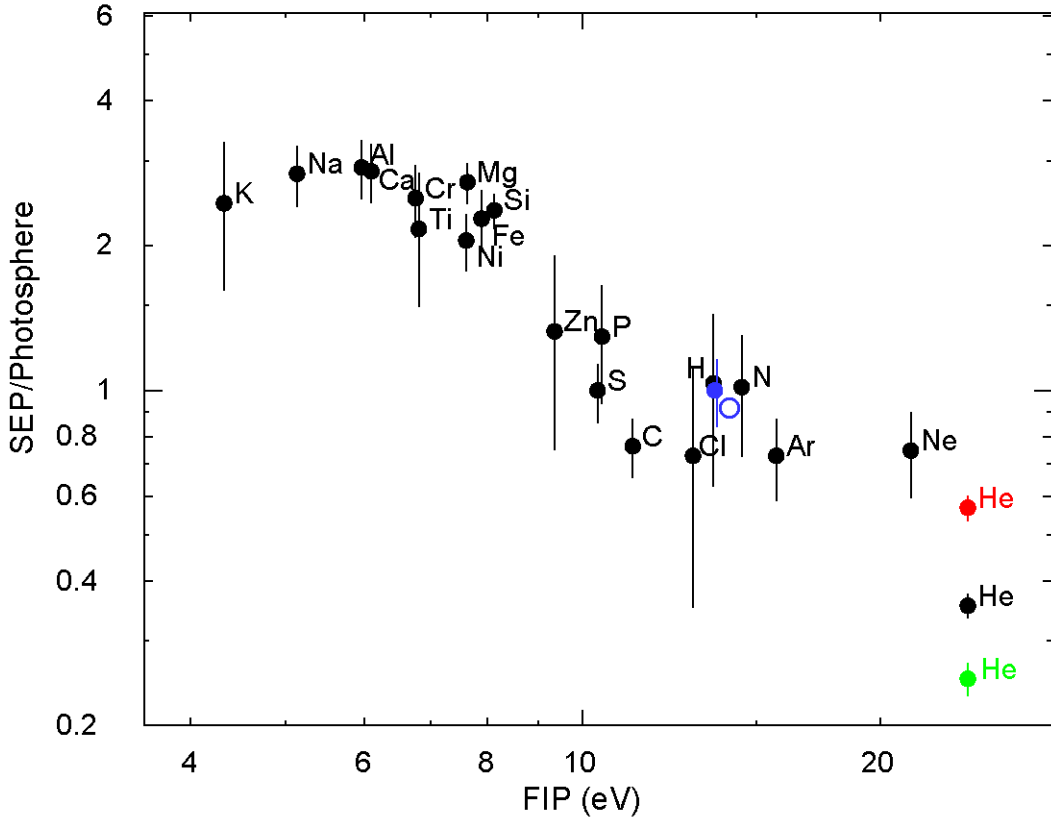


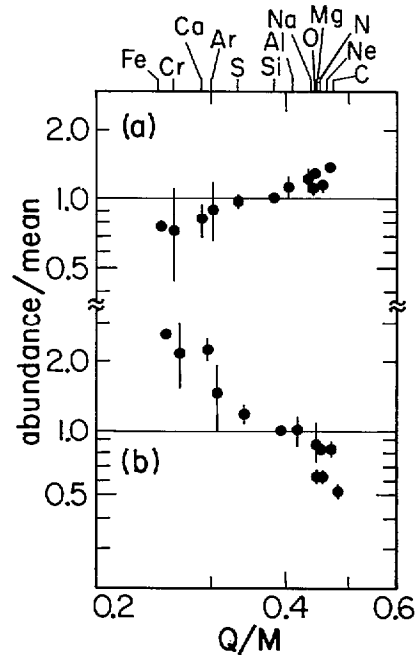
**Fig. 3** Element abundances from SEPs (Reames 2014, 2017a) are divided by photospheric abundances (Caffau et al. 2011, Lodders, Palme, and Gail 2009), normalized at O (blue). Abundances of He in three event regions correspond to He/O= 90 (red), 57 (black) and 40 (green) (see Section 4.1).

Direct measurement of the charge state  $Q$  for a variety of ions is difficult and is generally limited to energies below 1 MeV amu $^{-1}$ . The earliest measurement of  $Q$ -values for SEP ions (Luhn et al. 1984) were used with element abundances by Breneman and Stone (1985) to show SEP events with enhancements that either increased or decreased as a power-law function of  $Q/A$ . These events are shown in Figure 4. Values of  $Q$  of Fe from the measurements of Luhn (1984) showed a distribution peaking near  $Q_{\text{Fe}} \approx 14$  which corresponds to  $T \approx 2$  MK that controls the groupings of the elements along the top of Figure 4.

Upsetting the simple picture of impulsive and gradual SEP events is the fact that fast shock waves can also reaccelerate residual suprathermal ions left over from previous impulsive SEP events. In fact these suprathermal ions may even be preferentially accelerated. Mason, Mazur, and Dwyer (1999) first observed small, but significant, enhancements in  $^3\text{He}$  in SEP events that were otherwise large gradual events, and strong enhancements in  $^3\text{He}/^4\text{He}$  are now seen even in quiet periods (Desai et al. 2003; Bučík et al. 2014, 2015; Chen et al. 2015). These  $^3\text{He}$ -rich periods must involve many small jets in active regions producing many impulsive SEP events that are too small to be resolved individually. Shock waves passing through these regions may *preferentially* accelerate the suprathermal ions, depending upon the angle between the field  $B$  and the shock normal (Tylka et al. 2005; Tylka and Lee 2006). Quasi-perpendicular shocks may preferentially accelerate the faster suprathermal ions that can overtake the shock more

easily from downstream. A complex variation of abundance ratios, such as Fe/C, occurs especially at high energies  $> 10$  MeV amu $^{-1}$  where spectral breaks depend upon both the shock geometry and  $A/Q$ , which differs between the ambient and the suprathermal ions (Tylka et al. 2005; Tylka and Lee 2006). These reaccelerated impulsive suprathermal ions can have the spectra and intensities of shock acceleration, seen in other gradual SEP events, but the somewhat-diluted abundances of impulsive SEP events.

**Fig. 4** The dependence of elemental abundances on the charge-to-mass ratio  $Q/M$  (our  $Q/A$ ) of the elements is shown for two large SEP events by Breneman and Stone (1985) using values of  $Q$ -values measured by Luhn et al. (1984).



The association of gradual SEP events with CME-driven shock waves began with the 96% correlation between large SEP events and fast, wide CMEs (Kahler et al. 1984), and the broad spatial distribution of abundances (Mason, Gloeckler, and Hovestadt 1984), and continued with shock theory (Lee 1983, 2005; Zank, Rice, and Wu 2000; Zank, Li, Verkhoglyadova 2007; Ng and Reames 2008), reviews of properties (Gosling 1993, Reames 1999, 2013, 2015, 2017a; Kahler, 1992, 1994, 2001; Cliver, Kahler, and Reames, 2004; Cliver and Ling, 2007; Gopalswamy et al., 2012; Mewaldt et al. 2012; Lee, Mewaldt, and Giacalone, 2012; Cliver 2016; Desai and Giacalone 2016) and the detailed spatial CME studies of Rouillard et al. (2011, 2012, 2016).

### 2.3 What about flares?

Solar flares exist precisely because energetic particles in them are magnetically trapped. Without containment there would be minimal flash and X-rays; energetic charged particles would mostly be magnetically mirrored away from the Sun with minimal flash, as seen in jets where a small trapping region does exist (Shimojo and Shibata 2000; Reames 2002). Particles accelerated during magnetic reconnection on closed loops in flares scatter into the loss cone and plunge into the low corona where they interact in the denser matter and come to rest. Electron bremsstrahlung produces hard X-rays, and energetic ions undergo nuclear reactions producing  $\gamma$ -rays and neutrons that escape into space, but the ions do not. As energetic particles lose energy and stop in the dense

plasma, their energy deposit produces heating up to 10 – 20 MK and the hot plasma evaporates back up into the loops, causing the flash. Analysis of  $\gamma$ -ray lines from large flares suggests that the accelerated “beam” is  $^3\text{He}$ -rich (Mandzhavidze et al. 1999; Murphy, Kozlovsky, and Share 2016) and Fe-rich (Murphy et al. 1991), just like the impulsive SEP events that escape into space from jets. However, although  $^2\text{H}$ ,  $^3\text{H}$ , Li, Be, and B secondary ions are produced in flares, just as they are in the GCRs, these charged secondary ions cannot escape the flares. Nor can the primary ions. Even during Carrington’s (1860) first observation of a flare, he was “surprised … at finding myself unable to recognize any change whatever as having taken place.” The fields maintain their shape. Modern instruments allow measurement of the reconnection magnetic flux and a recent data base contains reconnection flux for 3137 solar-flare ribbon events (Kazachenko et al. 2017). However, large reconnection events lacking fast shock waves produce beautiful flares, but *no* SEPs (Kahler et al. 2017). Flares require containment by closed magnetic fields and disrupt those fields very little; the energy of particles accelerated in flares is dissipated by heating in the footpoints and loops and the particles are not released into space.

In principle,  $^3\text{He}$ -rich, Fe-rich, gradual events might have been seeded by flares, but the SEPs are too cool, 3 MK, and they have no nuclear-reaction fragments. As stated previously, none of the secondary ions expected from reactions are seen in space. Despite the enhancements of  $^3\text{He}$ , the isotopes  $^2\text{H}$  and  $^3\text{H}$  are not observed in SEPs. Limits on Be/O or B/O in large SEP events are  $<2 \times 10^{-4}$  and Li/O  $< 0.001$  (e.g. McGuire, von Rosenvinge, and McDonald 1979; Cook, Stone, and Vogt 1984). Furthermore, we do not see hot plasma. At 20 MK, Ne, Mg, and Si would be fully ionized and have  $A/Q = 2$ , like O. In gradual SEP events we do see plasma at  $\sim 3$  MK that is consistent with reacceleration of impulsive suprathermal ions from jets. These events are characterized by enhancements of Ne/O, unlikely for fully ionized Ne and O.

Furthermore, the classical magnetic topology of eruptive events suggests that major flaring produced by reconnection associated with the ejection of a CME would occur *beneath* or *behind* the CME in eruptive flares. If we wanted to look for residue from a flare among SEPs, we should look late in an event, *after* passage of the CME, for Be/O and B/O, for unenhanced Ne/O and Mg/O, and for a source plasma temperatures above 10 MK. Any small leakage of SEPs from flares is apparently dwarfed by SEPs accelerated at the CME-driven shock that have filled the reservoir (e.g. Reames 2013, 2017a) behind the shock.

Without containment there would be no flare. That containment prevents us from seeing SEPs accelerated at reconnection sites in flares. However, we do often see the ions from reconnection events that produce jets on open field lines nearby. There certainly may be events involving reconnection on *both* open and closed field lines. In those events acceleration on closed field lines produces a flare, while acceleration on open field lines produces a jet and the SEPs that are visible in space, but abundances show that the open and closed regions are not connected and do not communicate. Logically, it is not possible for the reconnection of closed field lines with other closed field lines to produce open field lines. There is simply no evidence of a flare contribution to SEPs.

## 3 Ionization States and Temperatures

### 3.1 Direct and Geomagnetic Measurement

The earliest direct measurements of ionization states (Luhn et al. 1984, 1987) provided a clear difference between gradual and impulsive events. On average, gradual events had  $Q_{\text{Fe}} = 14.1 \pm 0.2$  and  ${}^3\text{He}$ -rich events had  $Q_{\text{Fe}} = 20.5 \pm 1.2$  with wide distributions in individual events. The value for impulsive events was sometimes interpreted as originating in hot solar flares. However, it was later found that the value varied with ion energy as expected from the equilibrium obtained by passing the ions through a small amount of matter (DiFabio et al. 2008), consistent with sources below about  $1.5 \text{ R}_\odot$ . The matter traversed is not adequate to cause significant energy loss for the heavy elements, since their power in  $A/Q$  (Figure 2) has not been disrupted, even at very high  $Z$ .

The higher intensities and energies in gradual events permitted using deflection in the geomagnetic field to measure charge states (Leske et al. 1995) at  $15 - 70 \text{ MeV amu}^{-1}$  where the average  $Q_{\text{Fe}} = 15.2 \pm 0.7$ . Meanwhile, Tylka et al. (1995) found  $Q_{\text{Fe}} = 14.1 \pm 1.4$  at  $200 - 600 \text{ MeV amu}^{-1}$ . More recently, Klecker (2013) summarized mean values of  $Q_{\text{Fe}}$  for gradual events as being in the range from 10–14. These values are consistent with coronal temperatures of  $\sim 1.2 - 2.5 \text{ MK}$ , varying from event to event.

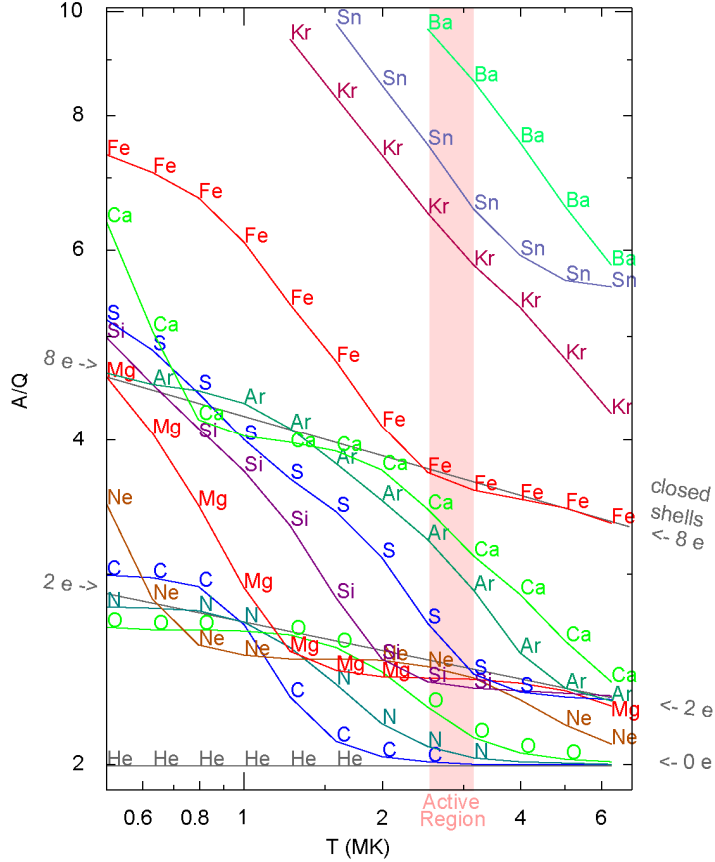
### 3.2 Inferring Temperatures from Abundances

The use of abundances alone to imply temperatures began when Reames, Meyer, and von Rosenvinge (1994) noted that He, C, N, and O in impulsive SEP events all had coronal abundances, as in the average of gradual events, thus they were probably all fully ionized and had the same value of  $Q/A = 0.5$ . Meanwhile, Ne, Mg, and Si all had very similar enhancements while the enhancement of Fe was larger. O is fully ionized at a temperature of  $T > 3 \text{ MK}$ , while Ne, Mg, and Si have closed shells of two orbital electron with similar values of  $Q/A \sim 0.43$  for  $2.5 < T < 4 \text{ MK}$ . In this temperature range,  $3 < T < 5$ , Fe has  $Q/A \sim 0.28$ . Using tables of  $Q$  vs.  $T$ , mainly from Arnaud and Rothenflug (1985), the pattern of abundances suggested this temperature region.

With more accurate measurements it became clear that the enhancements of Ne/O  $> \text{Mg}/\text{O} > \text{Si}/\text{O}$ , opposite the expected ordering in  $Z$ , which occurs for the respective values of  $A/Q$  at  $T = 2.5 - 3.2 \text{ MK}$  (Reames, Cliver, and Kahler 2014a). This together with the availability of enhancements for elements  $34 \leq Z \leq 82$  led to the plot of enhancement vs.  $A/Q$  in Figure 2.

The theoretical values of  $A/Q$  vs.  $T$  for elements that we use to derive temperatures are shown in Figure 5. Values of average  $Q$  vs.  $T$  for elements up to Fe are from Mazzotta et al (1998); those for typical elements above Fe come from Post et al (1977). The pink “active region” band in the figure marks the region where the observed pattern of element enhancements in impulsive SEP events matches the pattern of  $A/Q$ ; the  $A/Q$  values used in Figure 2 come from this band in Figure 5.

**Fig. 5**  $A/Q$  is shown as a function of the theoretical equilibrium temperature for elements named along each curve. Data are from Mazzotta *et al.* (1998) up to Fe and from Post *et al.* (1977) above. Points are spaced every 0.1 unit of  $\log_{10} T$ .  $A/Q$ -values tend to cluster in bands produced by closed electron shells; those with 0, 2, and 8 electrons are shown, He having no electrons. Elements move systematically from one band to another as temperatures change. The shaded pink region corresponds to active-region temperatures found for impulsive SEP events.

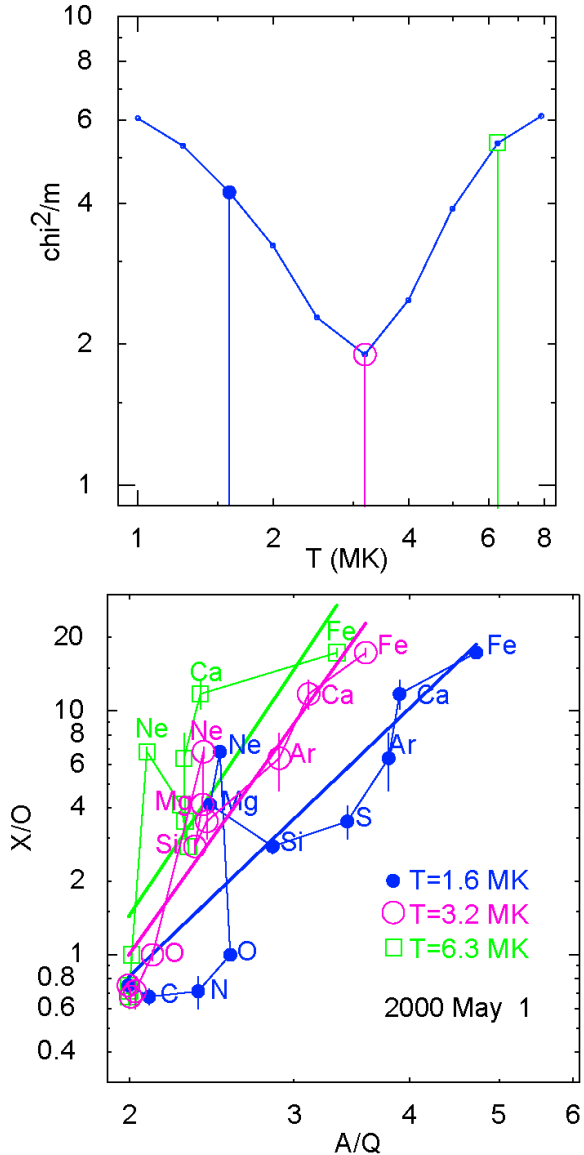


### 3.2.1 Impulsive SEP events

If we wish to determine a temperature for an individual SEP event, we simply fit the observed abundance enhancements *vs.* the  $A/Q$ -values at *each* temperature that could be of interest and record the value of  $\chi^2/m$  *vs.*  $T$ , where  $m$  is the number of degrees of freedom of the fit, i.e. the number of elements measured minus two. The best fit and corresponding temperature for each time are chosen at the minimum value of  $\chi^2/m$ .

Figure 6 shows data and power-law least-squares fit lines using  $A/Q$ -values at three temperatures for the impulsive SEP event of 1 May 2000. This event has been studied extensively in other respects (e.g. Reames, Ng, and Berdichevsky 2001; Kahler, Reames, and Sheeley 2001; Reames, Cliver, and Kahler 2014a). The best fit at 3.2 MK (red circles), seen in the lower panel of Figure 6, is somewhat distorted by the high value of Ne/O. High Ne/O is common in impulsive SEP events, but these events may also have high non-thermal variations of  $\sim 30\%$  in other species, as well (Reames, Cliver, and Kahler 2015; Reames 2016b). Decreasing the temperature from 3.2 to 1.6 MK (blue filled circles), increases  $A/Q$  for N, and O, but not for He, and C, and increases  $A/Q$  for Si through Fe but not for Ne and Mg; this causes severe distortion. Increasing the temperature from 3.2 to 6.3 MK (green squares), moves Ne down toward O, despite its greater enhancement and reduces  $A/Q$  greatly for Ca, but not for Fe, again causing obvious distortion. These changes in  $A/Q$  can be followed in Figure 5. Intermediate values in  $T$  result in intermediate values of  $\chi^2/m$ .

**Fig. 6** Least-squares power-law fits are shown for the impulsive SEP event of 1 May 2000. The lower panel shows data and fits of element abundance enhancements, relative to coronal values,  $X/O$  as a function of  $A/Q(T)$  for three selected temperatures. The observed values of  $X/O$  do not change with temperature. The upper panel shows  $\chi^2/m$  vs.  $T$  for fits at ten temperatures with values for the three selected fits highlighted with the corresponding symbol. The value of  $\chi^2/m$  for the best fit at  $T = 3.2$  MK remains above 1 largely because of the excess enhancement of Ne, but the fits become much worse and the data patterns are distorted as the assumed temperatures are raised or lowered.



The original study of 111 individual impulsive SEP events (Reames, Cliver, and Kahler 2014b) found 108 events had source plasma temperature minima of either 2.5 or 3.2 MK. A subsequent study (Reames, Cliver, and Kahler 2015) found some variation when weighting for the fits allowed for non-thermal variations up to 30% in quadrature with the statistical error, but a search found a dearth of events with abundance patterns that would be expected outside the 2 – 4 MK range. Individual impulsive SEP events do not stray far from the average.

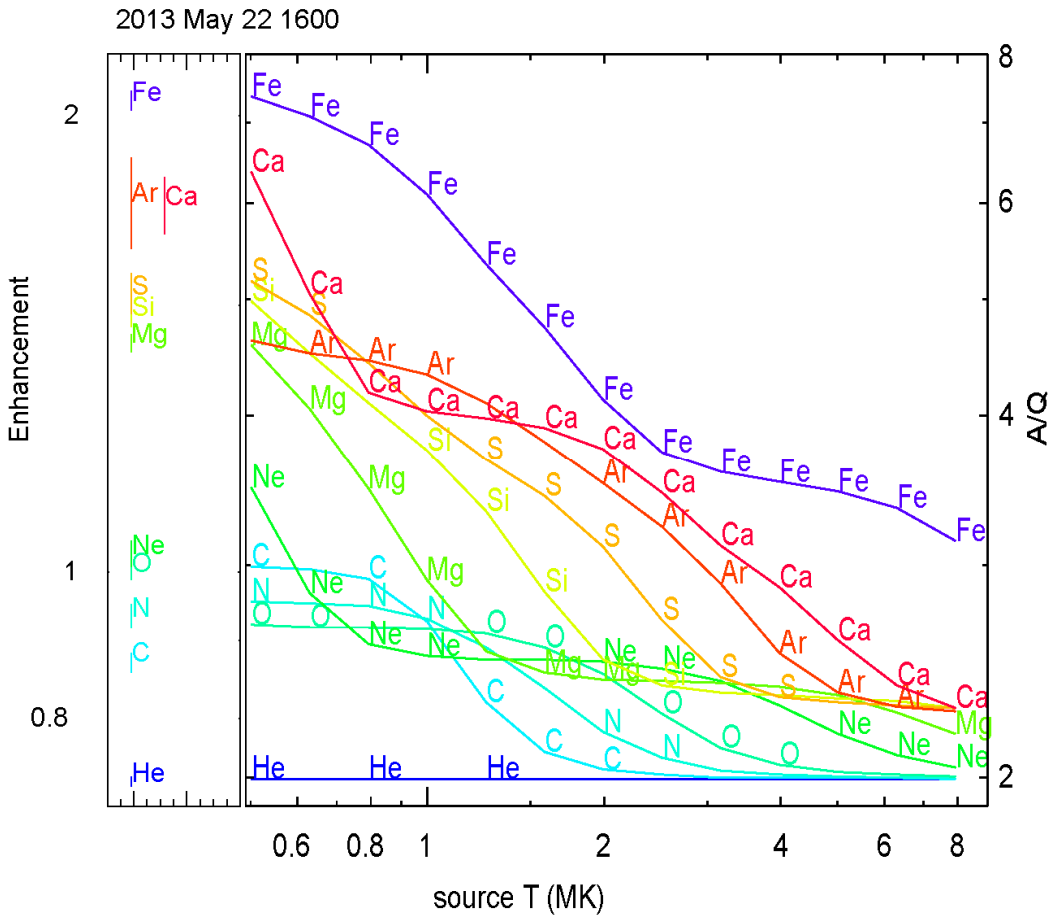
### 3.2.2 Gradual SEP Events

The observations of Breneman and Stone (1985), shown in Figure 4, provided the first strong evidence of a power-law dependence of abundance enhancements on  $A/Q$ , but the possible effect of temperature dependence of  $Q$  on the pattern of elements at the top of the plot in Figure 4 was not fully appreciated. In subsequent years, direct and geomagnetic measurements of  $Q$  became available that began to show the variability of

$Q_{Fe}$  and the temperatures that it implied. However, these measurements soon became less common and systematic studies of large samples of events were rare.

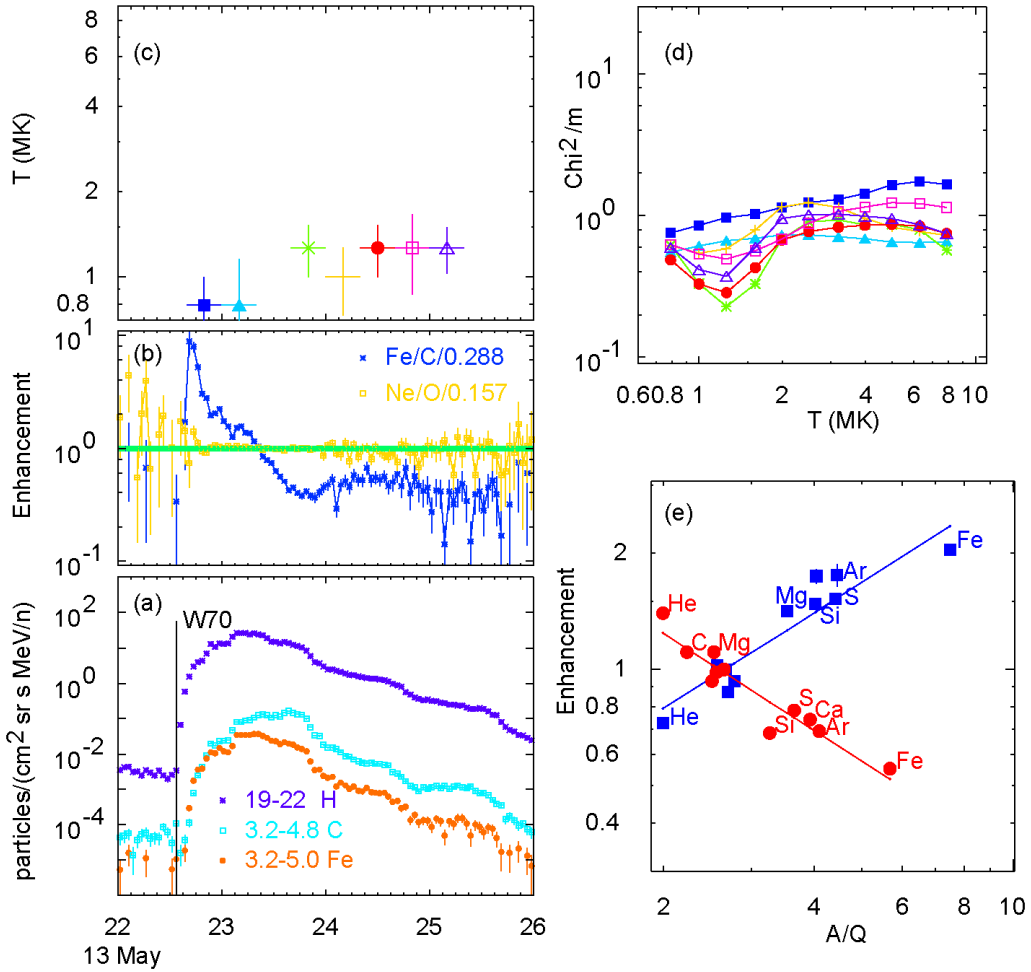
The success of the measurements of a large sample of impulsive SEP events using abundance enhancements *vs.*  $A/Q$  suggested the use of the same technique for gradual SEP events and it was shown that a power-law dependence of abundance enhancements upon  $A/Q$  was expected from diffusion theory (Reames 2016a, 2016b). Gradual events show a much wider span of temperature. The higher intensities also allow us to measure temperatures as a function of time during an event.

Figure 7 compares the observed pattern of enhancements early in the event of 22 May 2013 with a plot of  $A/Q$  *vs.*  $T$ . Unlike the pattern of elements in impulsive events, here C, N, and O have moved well above He to approach Ne, while Mg, Si, and S have moved far above Ne near Ar and Ca. We can almost judge the temperature by inspection from the pattern of abundance enhancements. We could scale He and Fe to match the spread at some other  $T$ , but the pattern of the intermediate elements would not fit.



**Fig. 7** The left panel shows observed enhancements in element abundances at *Wind* during the interval 1600 – 2400 UT 22 May 2013. The right panel shows  $A/Q$  *vs.*  $T$  for various elements, as in Figure 5. The groupings of enhancements match those in  $A/Q$  near 0.6 – 0.8 MK. Compared with impulsive events, here C, N, and O have moved above He to join Ne while Mg, Si, and S have left Ne approaching Ar and Ca (Reames 2016a).

A more complete analysis of this SEP event of 22 May 2013, in Figure 8, shows the deduced temperature dependence in 8-hr intervals throughout the event in panel (c).



**Fig. 8** Analysis of the 22 May 2013 gradual SEP event shows typical (a) intensities and (b) enhancements *vs.* time, (c) resulting temperatures *vs.* time, color coded, (d)  $\chi^2/m$  *vs.*  $T$  for each time, and (e) best fits of enhancement *vs.*  $A/Q$  at two selected times, early (blue square) and late (red circle). Either enhancement or suppression of abundances may be used to determine  $T$ , as shown in (e). Temperatures remain fairly constant throughout most events (Reames 2016a).

There are seven time intervals in the event in Figure 8. For each time interval, least-squares fits of enhancement *vs.*  $A/Q$  are done, using *each* of the 11 temperatures to determine  $A/Q$ -values. The resulting  $\chi^2/m$  is plotted *vs.*  $T$  as in panel (d) of Figure 8; the minimum value of  $\chi^2/m$  determines the best  $T$  for that time.

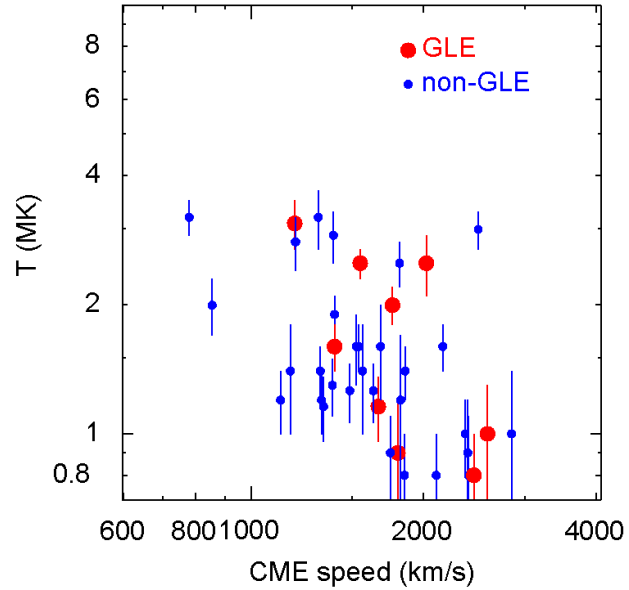
For example, the fifth time interval, at 0800 – 1600 on 24 May in Figure 8c, is shown as filled red circle. Fits using enhancements during this period and  $A/Q$ -values at *each* temperature result in the  $\chi^2/m$  *vs.*  $T$  curve of filled red circles in panel (d). This curve has a minimum at  $T = 1.26$  MK, which is then plotted as a filled red circle in panel (c) and the best fit line of enhancement *vs.*  $A/Q$  at that temperature is shown along with the points for each element as filled red circles in panel (e).

Note that one time interval has been skipped on 23 May in Figure 8 where the enhancement in Fe/O  $\approx 1$  in panel (b). When there is neither enhancement nor suppression, the power-law is flat, any  $A/Q$  will fit, and we cannot determine a temperature. When abundances are nearly coronal we find uncertain or ambiguous

values of  $T$  – there has not been enough scattering to alter the coronal abundances. Large enhancements or suppressions provide the best temperatures.

In a study of 45 gradual SEP events, 11 events (24%) had temperatures of 2.5 – 3.2 MK just like impulsive events (Reames 2016a). These have been understood as events that are dominated by reacceleration of residual suprathermal ions from impulsive SEP events. Event temperatures have no strong dependence on properties, such as CME speed, as shown in Figure 9, nor would we expect any. Data in the figure show an unweighted correlation coefficient of -0.49. GLEs are distinguished in the figure but apparently they have no special significance.

**Fig. 9** Temperatures of the source plasma in gradual SEP events are shown vs. speed of the driving CME. GLEs, emphasized in red, are unremarkable (Reames 2016a, 2016c).



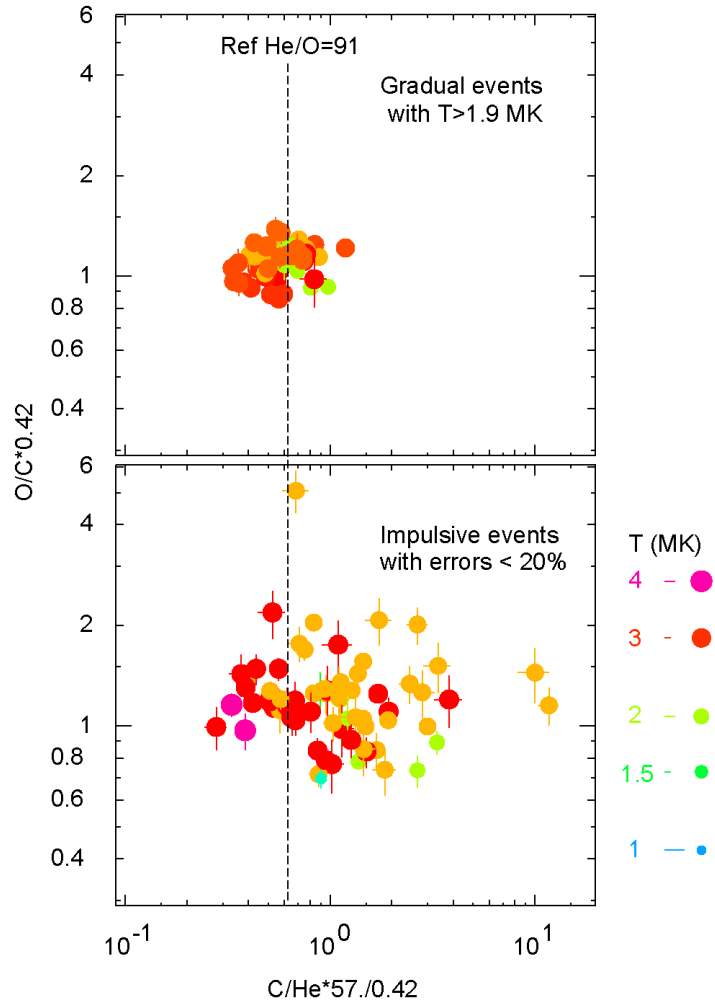
### 3.2.3 Comparing Impulsive and Gradual Events

Since we now have temperatures for both impulsive and gradual events, it is possible to compare properties of the two in the same temperature range, especially at high temperatures where He, C, N, and O are all likely to be fully ionized so that their relative abundances cannot be altered by either acceleration or transport.

Figure 10 shows a comparison of enhancements of O/C vs. C/He for impulsive (lower panel) and gradual (upper panel) SEP events, with coronal normalization values shown along the axes. The impulsive events are limited only by removal of events with large statistical errors. Gradual events include all 8-hr intervals during events with  $2 \leq T \leq 4$  MK.

Note that the gradual events in Figure 10 are tightly distributed while the impulsive events have a large spread with non-thermal errors that exceed the statistical errors shown. If these  $\sim 3$  MK gradual events are produced by shock reacceleration of suprathermal ions from impulsive SEPs from jets, they must average over the output from many small jets to reduce the non-thermal variance. As we noted previously, strong enhancements in  $^3\text{He}/^4\text{He}$  are seen even in quiet periods (Desai et al. 2003; Bučík et al. 2014, 2015; Chen et al. 2015). These  $^3\text{He}$ -rich periods must involve many small jets in active regions producing many impulsive SEP events that are too small to be resolved individually. Shock waves passing through these regions would average a seed population from many impulsive events, diluted by some ambient coronal plasma.

**Fig. 10** Enhancements of O/C vs. C/He are compared, for measurements in gradual SEP events with  $T > 1.9$  MK (upper panel) and for impulsive SEP events with  $< 20\%$  errors (lower panel).  $T$  is indicated by the size and color of the symbols. Both panels are plotted on the same scale to show differences in the distribution size. The median of the distribution of C/He for the gradual events, shown as a dashed line, implies a reference coronal value for He/O of 91 rather than 57 (Reames 20016b), i.e. He/O = 91 normalized the dashed line to 1.0.



Another feature of Figure 10 is the offset of the mean enhancement of C/He for the hot gradual events from one. Since C must be fully ionized at the temperatures in these events, this means we must have the wrong “coronal” or reference value for He. Instead of He/O of 57, as assumed, these hot events would require He/O=91. Note the effect of the higher He/O value as the red circle on the FIP plot in Figure 3.

As we move down in temperature for the cooler gradual events, O is no longer fully ionized, and as it is enhanced, He/O decreases. Thus averaging He for all gradual events gives a lower value of He/O. How much do reference abundances vary?

## 4 Reference Abundance Variations

The SEP coronal abundances we have used to measure enhancements in both impulsive and gradual events have been derived by averaging over many gradual SEP events, either in solar cycle 21 (Reames 1995) or in cycles 23 and 24 (Reames 2014). This assumes that when differences in particle scattering produce enhancements at one time in one location it will cause depressions at another time and location. Is there a single “coronal” abundance for each element?

## 4.1 Helium Abundance Variations

Variations of He/O are seen in the solar wind as functions of time and of solar-wind speed (Collier *et al.* 1996; Bochsler 2007; Rakowsky and Laming 2012) and large variations are seen in H/He with phase in the solar cycle (Kasper *et al.* 2007). Unfortunately, we cannot deduce coronal H from SEPs since H strongly controls its own wave generation and scattering (e.g. Reames, Ng, and Tylka 2000; Ng, Reames, and Tylka 2003), among other problems. Are the solar wind abundance variations a property of the solar corona itself, or only related to the formation of the solar wind? Could these, or other, coronal variations also be measurable in SEPs? Evidence in Figure 10 that the “hot” events could have a reference He/O=91 rather than 57, strongly suggests that this is possible.

In some gradual SEP events there is also evidence that the observed value of the enhancement in He/O does not fit the power-law dependence on  $A/Q$ . Three examples are shown in Figure 11. For the event in panel (a) He falls below the fits; the fit and  $\chi^2$  would be improved using a *reference* He/O  $\approx 40$ . For the event in panel (c), He fall well above the fit lines; the fits and  $\chi^2$  would be improved using a reference He/O  $\approx 90$ . The event in panel (b), *and for the event in Figure 8*, reference He/O = 57 seems just right.

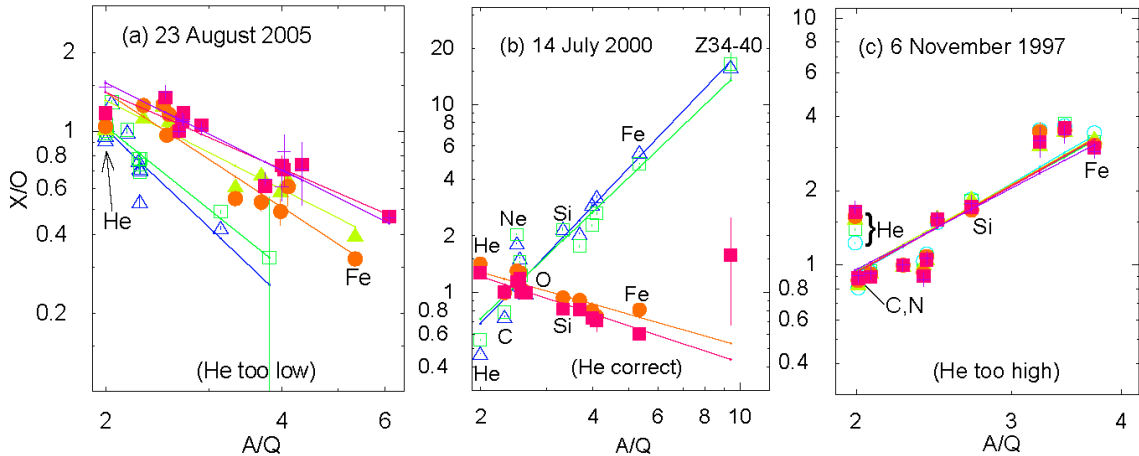
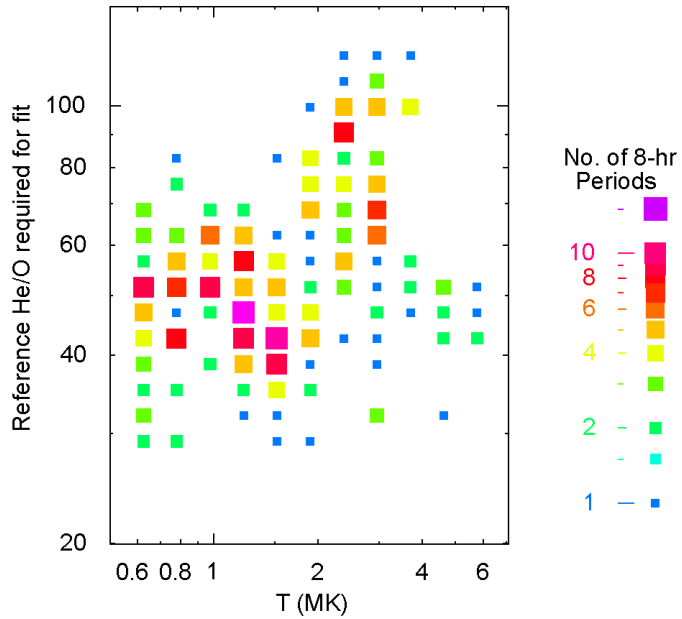


**Fig. 11** Least-squares power-law fits of enhancement vs.  $A/Q$  are shown during three gradual SEP events. All He enhancements shown are based upon a reference value of He/O = 57. In (a) the event of 23 August 2005, He falls below the fit lines; in (b) the event of 14 July 2000, both enhancements and suppressions appear consistent, and in (c) the event of 6 November 1997 He falls well above the fit (based on fits in Reames 2016a).

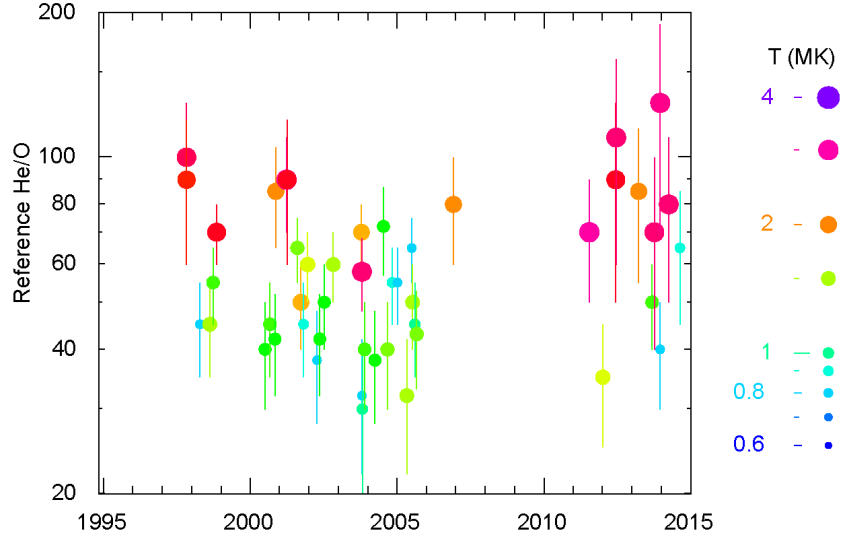
For each of the 8-hr periods studied in the gradual SEP events, suppose we calculate the value of the reference He/O that would be required to bring the He enhancement to the fit line. Figure 12 is a histogram of the number of occurrences of each reference He/O as a function of  $T$ . There is clearly a temperature dependence of the *reference* He/O value, in addition to the power-law transport.

**Fig. 12** A histogram of the reference value of He/O that would be required to bring the He enhancement onto the best-fit power-law is shown vs.  $T$ . The histogram includes each 8-hr period during gradual events. Temperatures in the 2.5–3.2 MK active-region intervals require higher values of the underlying coronal He/O ratio (Reames 2017c).



The reference value of He/O is quite constant during events and its variation in events throughout the solar cycle is shown in Figure 13. Since the abundances of the hotter gradual events are actually determined from the impulsive suprathermal ions in the seed population, the higher value of He/O may be determined deeper in the corona.

**Fig. 13** The estimated coronal value of He/O required for each gradual SEP event is shown vs. time, with the source plasma temperature indicated as the size and color of the circle (Reames 2017c).



## 4.2 Abundances of Heavier Ions

It is possible to treat the abundances of heavier ions just as we have treated the abundances of He, *i.e.* to ask what reference value would bring the enhancement to the power-law fit line of the other elements. However, other elements show no significant variations. For C/O, for example, mean values show essentially no temperature difference: derived coronal C/O =  $0.392 \pm 0.007$  averaged over SEP events with  $T = 2$ –4 MK and C/O =  $0.398 \pm 0.006$  for  $T < 2$  MK (Reames 2017c). However, this ratio for SEPs

never exceeds 0.50, nor approaches the mean value of  $C/O = 0.68 \pm 0.07$  in the solar wind (Bochsler 2009).  $C/O$  shows the largest significant difference between SEPs and the slow solar wind, a difference that has been unexplained, although a more recent measurement in the bulk solar wind does give  $C/O = 0.53 \pm 0.06$  (Heber *et al.* 2013). Why do SEPs and the slow solar wind disagree?

## 5 Coronal Abundances: SEPs and the Solar Wind

The lower panel in Figure 14 compares the average SEP element abundances (e.g. Reames, 2014, 2017a) with those of the slow or interstream solar wind (SW; Bochsler 2009) by showing the ratio of the two as a function of FIP. SEP abundances are those shown in Figure 3 and listed in Table 1, with  $He/O = 91$ . The upper panel shows both SEP and SW abundances relative to the photospheric abundances with the dominant element species from Caffau *et al.* (2011) and other elements from Lodders, Palme, and Gail (2009) just as in Figure 3. Data shown in Figure 14 are listed in Table 1.

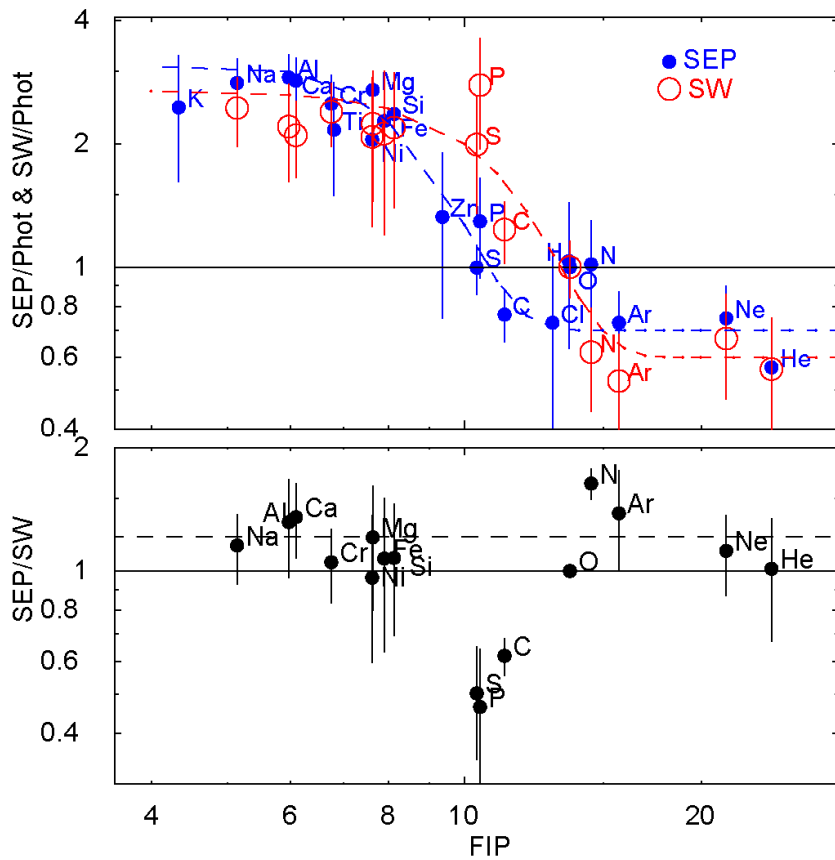


**Fig. 14** The upper panel shows the SEP/photospheric and Solar Wind (SW)/photospheric abundance ratios as a function of FIP. Dashed curves are empirical curves used to help show the trend of each data set. The lower panel shows the ratio of the “coronal” abundances from SEPs to those of the slow SW (Bochsler 2009), as a function of FIP. The dashed line suggests an alternate normalization. Data shown in Figure 14 are listed in Table 1.

Compared with the solar wind, SEP abundances of P, S, and C are low, and N is high, all other element abundances are consistent as shown in Figure 14. Apart from a small vertical shift based upon differences in the O normalization, the greatest difference between the SEP and SW abundances is a difference in the FIP of the transition from

low- to high-FIP abundance levels. One could argue that the transition from low- to high-FIP levels changes from  $\sim 10$  eV for SEPs to  $\sim 12$  eV for the SW, so that P and S tend to be high-FIP elements for SEPs but clearly low-FIP elements for the SW. This seems to require a completely different region of FIP processing for the two populations. Perhaps *the photosphere is cooler, on average, beneath regions producing SEPs, so that C, S, and P are neutral atoms there. The SW comes from hotter photospheric plasma, where S and P, at least, are ionized, and C is partially ionized.* This seems surprising until we realize that *CMEs, and certainly jets, are emitted near solar active regions that are above sunspots which have cooler plasma than elsewhere on the Sun.* Possibly SEP acceleration is more likely to occur above sunspots, while the source of the slow solar wind is more broadly distributed.

The coronal temperature is important if ions are much more easily swept up into the corona than neutral atoms as by the ponderomotive force of Alfvén waves (Laming 2004, 2009, 2015).

Certainly the temperature of the photosphere is not isothermal, in any case, and the width of the transition between low- and high-FIP abundance levels may itself attest to temperature variations across the sources of the ions. Thus, O may not be an ideal normalization for comparing SEPs and SW, since it is high-FIP for SEPs but transition for the SW. Perhaps a better normalization would be Ar and Ne (not He since SEP He varies) or the elements Mg, Si, and Fe; increasing all SW values by 15–20%, shown as the dashed line in the lower panel of Figure 14, greatly improves the agreement at asymptotically high and low FIP and amplifies the difference in the crossover.

Recently, extreme-ultraviolet (EUV) and X-ray spectroscopy observations near sunspots have shown regions with variations in the abundance ratios of Ar and Ca that sometimes even involve a reverse-FIP effect where Ar/Ca is enhanced (Doschek and Warren 2016, 2017). While this tends to support possible effects of a cooler environment, it is different in character from the SEP-SW differences above. In our case the amplitude of the FIP level difference varies little from SEPs to the SW; Ca/Ar =  $2.6 \pm 0.4$  in SEPs and  $2.6 \pm 0.7$  in the SW. These elements are not in the region of crossover from high to low FIP. The difference between the SEP and SW FIP patterns is almost entirely in the value of the crossover FIP.

The origins of SEP and SW ions have another important difference. The corona is weakly bound to the Sun by a collection of high closed magnetic loops that help to contain the plasma. A fast CME-driven shock wave driving through the corona can rapidly accelerate some of the local ions to MeV-energy SEPs. The *local magnetic fields are no longer strong enough to contain these new SEPs, so they easily escape*, beginning at about  $2 - 3$   $R_\odot$  (Reames 2009b). The *SW ions cannot sample these closed loops* unless they are eventually opened; SW ions must originate on field lines that are truly open to 1 AU and beyond. The open field lines may be much less likely to be rooted in the sunspots. In addition, high loops tied more closely to solar jets in active regions may help to trap impulsive suprathermal ions for later shock acceleration.

It is somewhat surprising that we never see evidence of SEPs with FIP-bias like that of the SW, since shocks *do* propagate even into the fast solar wind, (Kahler and Reames 2003, Kahler, Tylka, and Reames 2009). Perhaps the density of seed particles trapped in filaments and near active regions, coupled with cross-field diffusion in the shock front, swamps direct acceleration from the SW.

Table 1 Photospheric, SEP, and Spectroscopic Coronal Abundances.

	Z	FIP [eV]	Photosphere <sup>1</sup>	SEPs <sup>2</sup>	Interstream Solar Wind <sup>3</sup>
H	1	13.6	$1.74 \times 10^6$ <sup>*</sup>	$(\sim 1.57 \pm 0.22) \times 10^6$	–
He	2	24.6	$1.6 \times 10^5$	$91000 \pm 5000$	$90000 \pm 30000$
C	6	11.3	$550 \pm 76$ <sup>*</sup>	$420 \pm 10$	$680 \pm 70$
N	7	14.5	$126 \pm 35$ <sup>*</sup>	$128 \pm 8$	$78 \pm 5$
O	8	13.6	$1000 \pm 161$ <sup>*</sup>	$1000 \pm 10$	1000
Ne	10	21.6	210	$157 \pm 10$	$140 \pm 30$
Na	11	5.1	3.68	$10.4 \pm 1.1$	$9.0 \pm 1.5$
Mg	12	7.6	65.6	$178 \pm 4$	$147 \pm 50$
Al	13	6.0	5.39	$15.7 \pm 1.6$	$11.9 \pm 3$
Si	14	8.2	63.7	$151 \pm 4$	$140 \pm 50$
P	15	10.5	$0.529 \pm 0.046$ <sup>*</sup>	$0.65 \pm 0.17$	$1.4 \pm 0.4$
S	16	10.4	$25.1 \pm 2.9$ <sup>*</sup>	$25 \pm 2$	$50 \pm 15$
Cl	17	13.0	0.329	$0.24 \pm 0.1$	–
Ar	18	15.8	5.9	$4.3 \pm 0.4$	$3.1 \pm 0.8$
K	19	4.3	$0.224 \pm 0.046$ <sup>*</sup>	$0.55 \pm 0.15$	–
Ca	20	6.1	3.85	$11 \pm 1$	$8.1 \pm 1.5$
Ti	22	6.8	0.157	$0.34 \pm 0.1$	–
Cr	24	6.8	0.834	$2.1 \pm 0.3$	$2.0 \pm 0.3$
Fe	26	7.9	$57.6 \pm 8.0$ <sup>*</sup>	$131 \pm 6$	$122 \pm 50$
Ni	28	7.6	3.12	$6.4 \pm 0.6$	$6.5 \pm 2.5$
Zn	30	9.4	0.083	$0.11 \pm 0.04$	–

<sup>1</sup>Lodders, Palme, and Gail (2009)<sup>\*</sup>Caffau *et al.* (2011)<sup>2</sup>Reames (1995, 2014, 2017a)<sup>3</sup>Bochsler (2009)

Brooks, Ugarte-Urra, and Warren (2016) have identified regions of high FIP-level abundance differences on the Sun using spectral line measurements to determine Si/S abundance ratios which they show for the whole Sun. The Si/S ratio tends to be enhanced in the vicinity of active regions. While these measurements do indeed

determine regions of interest for SEP acceleration, they have much less relevance for the slow solar wind where Si and S are both low-FIP ions and their ratio does not measure FIP level differences. Si/S may show source regions for SEPs, but does not show the source region of the slow solar wind. A different choice of spectral lines, e.g. for Mg/Ne, if possible, might be a better indicator of the origin of the solar wind when compared with Si/S.

We consider the sketch of a possible magnetic configuration to produce the observed SEP-SW FIP differences in the Discussion section below.

## 6 Spatial Distributions – Multi-Spacecraft Observations

Now that we can use element abundances to measure source-plasma temperatures, we can study particle source properties with multiple spacecraft and address new questions. Do the SEPs at each longitude have a local origin? To what extent do particles from a common origin spread laterally across the face of a shock wave? We can compare SEP abundances observed over a broad longitude span at the *Wind* and the two STEREO spacecraft. Some basic properties of the events at STEREO, such as Fe/O spectral variations, peak intensities, and fluences have been studied recently by Cohen et al. (2014) and Cohen, Mason, and Mewaldt (2017).

Figure 15 shows an analysis of the interesting event of 31 August 2012 at *Wind* and STEREO B. The properties of the event at both spacecraft are seen in panels (a) and (b) while the resulting temperatures are seen in panel (c). The  $\chi^2$  curves for STEREO B in panel (d) show an early minimum at high  $T$  then transition to lower  $T$ , while those for *Wind* in panel (e) always minimize at low  $T$  throughout the event.

Early in the event, STEREO B, which is magnetically well-connected to the source, sees plasma at  $3.2 \pm 0.8$  MK while *Wind*,  $116^\circ$  to the west, sees  $1.6 \pm 0.2$  MK, as seen in Figure 15c. Figure 15f shows the change in the power-law fit at STEREO B with time. When the temperature at STEREO B declines on 3 September (panel (c)), all of the intensities (panel (a)) on both spacecraft are quite similar, suggesting that they are both in a reservoir region (e.g. Reames 2013, 2017a) behind the CME. Reservoirs function as a magnetic bottle behind a CME, where spatially uniform intensities decrease adiabatically with time as the CME expands, increasing the volume of the bottle. These observations suggest that the source of the plasma in the reservoir differs from that seen early in the event, i.e. the change in time is caused by a variation in space.

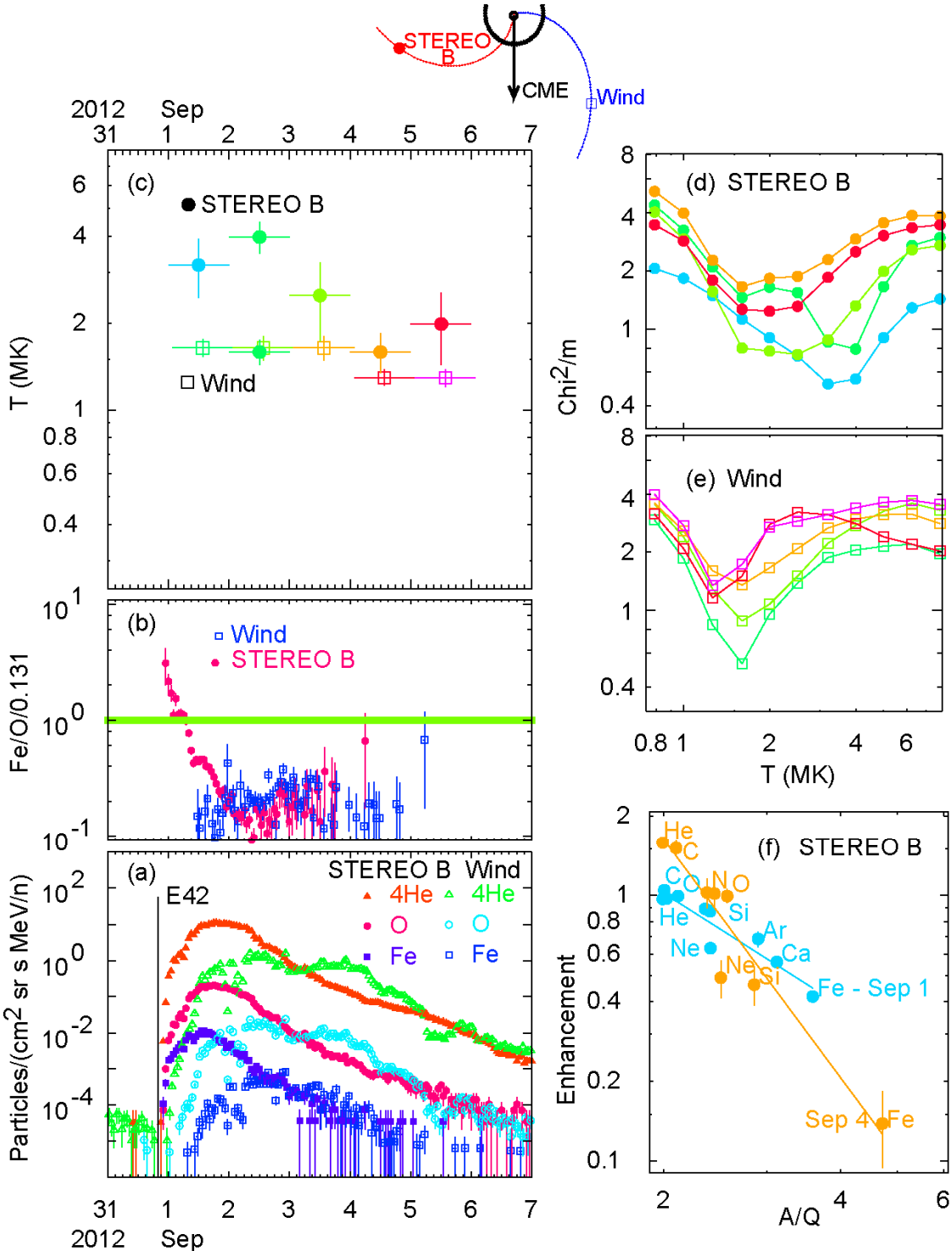
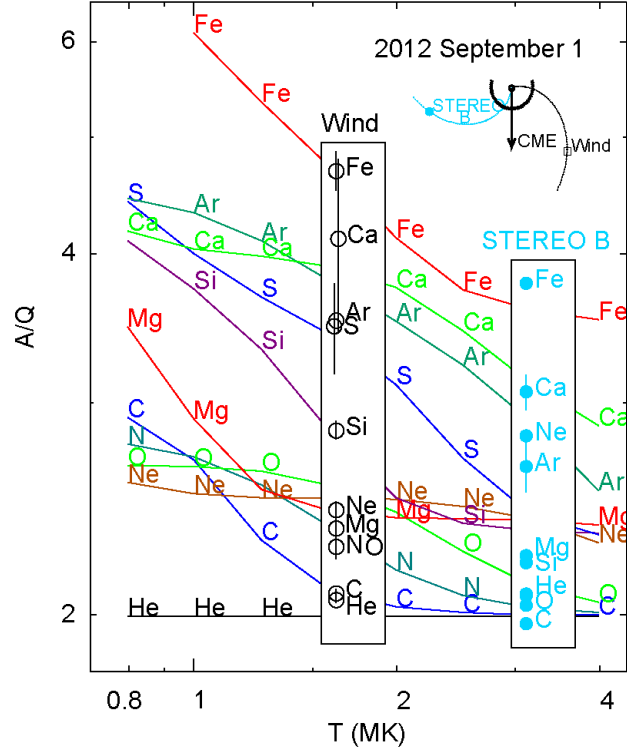


**Fig. 15** The 31 August 2012 SEP event is shown for STEREO-B (filled) and Wind (open symbols): (a) the intensities of He, O, and Fe vs. time, (b) the enhancements of Fe/O vs. time, (c) the derived source temperatures,  $T$  vs. time, (d and e)  $\chi^2/m$  vs.  $T$ , color coded for time, for (d) STEREO-B and (e) Wind, and, (f) enhancement vs.  $A/Q$  fits for early and late days at STEREO-B. The spacecraft locations relative to the CME are shown above (Reames 2017b)

It is possible to use the two parameters of each fit to map enhancements of each element into  $A/Q$ -space to see how the individual element abundances compare with expected  $A/Q$  values at the best-fit temperature. Figure 16 such a comparison on 1 September 2012 for enhancements at *Wind* and STEREO B.

**Fig. 16** Measured values of enhancements, X/O at *Wind* and STEREO-B on 1 September 2012, are mapped into the theoretical plot  $A/Q$  vs.  $T$  at 1.6 MK and 3.2 MK, respectively, using the best-fit parameters for each spacecraft. These measurements correspond to different source plasma temperatures at different locations in space, as shown in the inset, at the same time early in the SEP event (Reames 2017b).



The abundance enhancements at *Wind* match the pattern of  $A/Q$  quite well: He and C are fully ionized but N and O have joined Ne and Mg while Si and S have moved up. STEREO B, shows the impulsive pattern with He, C, N, and O all fully ionized (in fact, He should have been divided by 91 rather than 57 so it is not above C and O); however, Ne is overly enhanced relative to Mg and Si. Actually, of course, these are suppressions that decrease with  $A/Q$ , not enhancements (e.g. see Figure 15f) and there are other events with non-thermal variations in elements other than Ne. However, late in the event, the same anomaly in Ne/O is seen at both *Wind* and STEREO B, again suggesting a reservoir.

So far we only have one event with clear spatial variations in source temperatures. Three other events that were studied show possible variations, but temperature differences were not clearly resolved statistically (Reames 2017b).

## 7 Discussion

Our current understanding of impulsive SEP events is as follows: A steep power-law dependence of the average element abundance enhancements on  $A/Q$  is seen to be similar at low energy as  $(A/Q)^{3.3}$  (Mason et al. 2004) and higher energies as  $(A/Q)^{3.6}$  (Reames, Cliver, and Kahler 2014a), across the periodic table. This power law appears to be an expected consequence of scattering of ions in islands of magnetic reconnection (as found in particle-in-cell calculations by Drake et al. 2009) that occur on open magnetic field

lines in solar jets (Kahler, Reames, and Sheeley 2001) accompanied by slow, narrow CMEs without shocks (Reames, Cliver, and Kahler 2014a). Copious electron acceleration in the reconnection region leads to electron beams that produce type III radio bursts that have long been associated with these impulsive events that were first identified as  ${}^3\text{He}$ -rich events (Reames, von Rosenvinge, and Lin 1985; Reames and Stone 1986). The huge enhancements of  ${}^3\text{He}$  appear to be produced by resonant wave-particle interactions with electromagnetic ion-cyclotron waves that may be produced by the streaming electrons (Temerin and Roth 1992).

The electron temperature in the plasma that is accelerated in impulsive SEP events is  $\approx 3$  MK as determined from the pattern of ionization states  $Q$  consistent with the power law dependence upon  $A/Q$  (Reames, Cliver, and Kahler 2014a, 2014b). However, the reconnection region may occur below 1.5 solar radii, so that the ions traverse enough material after acceleration to strip them to equilibrium charge states that depend upon their energy (DiFabio et al. 2008), but the amount of material traversed is not enough to cause energy loss of the extremely high-Z ions, since that energy loss would have destroyed the power-law dependence on  $A/Q$ .

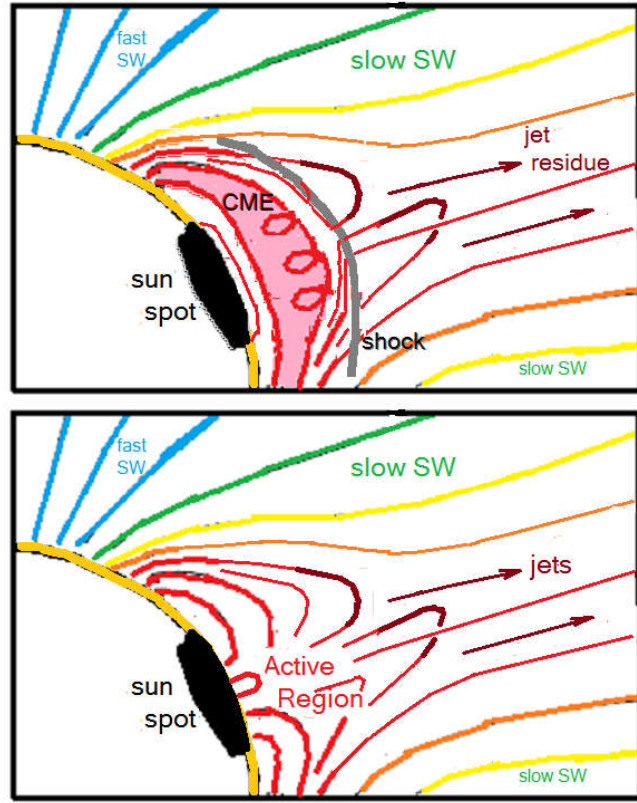
The average abundances, the power-law enhancements, and source plasma temperatures seem well defined for most events both above and below 1 MeV amu $^{-1}$ . However, there are a few small impulsive events with steep spectra that have unusual abundances, such as an unusual enhancement of N and especially of S (Mason, Mazur, and Dwyer 2002; Mason et al 2016), in one event S/O = 32. Rounded energy spectra of some of the heavy nuclei, near 0.1 MeV amu $^{-1}$  in these events, are similar to the rounded spectra of  ${}^3\text{He}$  rather than the power-law energy spectra of  ${}^4\text{He}$  or O (Mason et al 2016). These events are rare, about one per year, and most are too small to be measureable above 1 MeV amu $^{-1}$ . However, we do not understand these events, nor do we understand the source of the non-thermal abundance variations in impulsive events (e.g. Figure 10).

It is commonly known that impulsive SEP events occur in clusters (e.g. Reames, von Rosenvinge, and Lin 1985; Reames and Stone 1986; Reames 2000; Reames 2017a) while an observer is magnetically connected to a single active region on the Sun. Desai et al. (2003) found  ${}^3\text{He}$ -rich periods that were otherwise quiet that lasted for days. Multi-day and recurrent  ${}^3\text{He}$ -rich periods have been associated with active regions (Bučík et al. 2014, 2015; Chen et al. 2015). These periods are probably caused by many small jets each producing a  ${}^3\text{He}$ -rich SEP event that is too small to be resolved as an individual event. As we move toward smaller events, they become more numerous. A similar situation occurs with flares, where flare energy decreases, the number of flares per day increases as a power law. This observation led Parker (1988) to suggest that nanoflares were sufficient to heat the corona. Flares involve magnetic reconnection on closed field lines while jets are from reconnections on open field lines, so it seems plausible that “nanojets” might keep a basic level of  ${}^3\text{He}$ -rich material flowing from active regions. When the fast shock wave of a gradual SEP event passes above these active regions, it encounters a seed population that has averaged suprathermal ions over many jets so the non-thermal variations in abundance are small, as seen in Figure 10 (Reames 2016b). Averaging over just 10 impulsive events can reduce a 30% variation to 10%.

Figure 17 is a sketch of a possible configuration leading to different FIP dependence of SEP and SW abundances. Field lines from the active-region corona (red) connect to cool sunspots where C atoms are neutral and S and P are partially so. Red

field lines carry the SEP pattern of FIP. Field lines carrying slow SW (yellow, green) originate outside the active region where warmer photosphere outside sunspots ionizes S and P and some of the C to produce the FIP pattern of the slow SW (Figure 14). In the upper panel of Figure 17, a CME-driven shock wave accelerates material from the high corona above an active region, possibly including residual impulsive suprathermal ions from previous jets (enhanced in  $^3\text{He}$  and heavy ions), left-over bulk ejecta from jets (unenhanced), and other material from the high corona above the active region. Some regions of the shock wave in many gradual SEP events must sample only recently-formed high coronal loops, also with footpoints in sunspots, where the slowly-evolving He abundance has attained as little as half of its full value (Rakowski and Laming 2012; Laming 2015). As the CME and shock expand, both radially and laterally, with time they push aside the neighboring regions and even deflect streamers (Rouillard et al. 2011, 2012) spreading the SEPs over a wider longitude range.

**Fig. 17** Sketch of possible sources of SEPs and the SW. The lower panel shows an active region (red), with field lines connected to cool sunspots (black), from which solar jets emerge with an SEP-like FIP pattern. Field lines carrying the slow SW (yellow and green) diverge from warmer photosphere outside of active regions. The upper panel depicts a CME-driven shock wave (gray) that accelerates material from the high corona and residue from jets. Blue field lines track the fast SW from coronal holes have a photospheric source similar to the slow SW, but much less trapping and a weaker FIP effect. Newly-formed He-poor coronal regions on the fringe of active regions are not shown.



The average element abundances in gradual SEP events are a measure of element abundances in the active-region solar corona. The acceleration begins at an altitude of 2 – 3 solar radii (Reames 2009a, 2009b). These abundances are comparable with those from spectral line measurements of corona and with those of the slow solar wind (Schmelz, 2012). However, the origin of the differences between the SEP and SW abundance is *not* in the corona, where the SEP ions are accelerated, it must lie in the cooler photosphere of the sunspots that underlie the active regions where most of the SEP acceleration takes place, altering the location of the crossover on a FIP plot as in Figure 14.

Gradual SEP events involve shock acceleration of the ions from the ambient solar corona at  $\sim 1 - 2$  MK or the acceleration of remnant suprathermal ions at  $\sim 3$  MK from impulsive SEP events above active regions as just described. The use of the  $A/Q$ -dependence of abundance enhancements works well in the energy region of a few MeV  $\text{amu}^{-1}$ . At higher energy, usually above  $\sim 10$  MeV  $\text{amu}^{-1}$ , the spectra soon break downward and steepen, introducing abundance variations that depend upon the seed population and the shock geometry (e.g. Tylka and Lee 2006). Below 1 MeV  $\text{amu}^{-1}$  the spectra and abundances depend more strongly upon transport in large events and the shocks sample material far out into the solar wind, but low energies have been ideal for the study of impulsive SEP events (Mason 2007).

In one case, measurement at different longitudes in a gradual SEP event showed 3.2 MK source plasma at one well-connected spacecraft but 1.6 MK source plasma at another,  $116^\circ$  away. In a reservoir region behind the CME temperatures approach 1.6 MK at both spacecraft (Figure 15) and a similar pattern of abundances. Other events show possible, but less definite, temperature variations along the shock. A larger sample of events would be helpful.

Finally, we should note that using abundances to measure temperatures is not a substitute for other direct measurements. The SEP sources are not isothermal, yet we are only able to derive a single temperature. Direct measurements give us important information on the *distribution* of charge states which is also important for understanding the physics. The transport of  $\text{Fe}^{+10}$  is much different from that of  $\text{Fe}^{+20}$ ; in such a mixture, the  $\text{Fe}^{+10}$  would forge ahead, leading to a substantial increase in  $Q_{\text{Fe}}$  and in  $T$  with time. If we could follow it, the time dependence of  $\text{Fe}^{+10}/\text{Fe}^{+20}$  would behave much like Fe/O that we observe today. In some cases, perhaps, the differences within an event could be as large as that between events of greatly different temperatures. We need to know this, and direct measures of  $Q$  are still very important.

## 8 Summary

Early observers began the study of SEPs with the largest events, from the ground where no SEP abundance measurements are possible. Measurements in space soon began to distinguish the unusual abundances in the  ${}^3\text{He}$ -rich events and the FIP-related coronal-abundance basis of the gradual events. Abundance enhancements that vary as  $A/Q$  in both event types have led to the use of abundances to measure ionization states and temperatures. The following properties of SEPs are derived from abundances:

- 1) Lack of detectable abundances of  ${}^2\text{H}$ ,  ${}^3\text{H}$ , Li, Be, and B show that SEPs must not have escaped from the nuclear reactions that are seen to occur in solar flares.
- 2) Average element abundances in *gradual* SEP events provide a measure of coronal abundances.
- 3) Relative to coronal abundances, enhancement in element abundances in *impulsive* SEP events have a strong power-law dependence on  $A/Q$ , varying 1000-fold from He to Pb, produced during acceleration in islands of magnetic reconnection in solar jets.
- 4) 1000-fold increases in  ${}^3\text{He}/{}^4\text{He}$  are produced in *impulsive* SEP events by resonant wave-particle interactions in the jet sources.

5) Power-law dependence of abundance enhancements on  $A/Q$ , produced by either acceleration or transport, can be used to determine  $Q$ -values and source plasma temperatures. This technique may be used wherever abundance enhancements or suppressions are observed, including remote spacecraft.

6) Residual suprathermal impulsive SEP ions flowing from multiple jets in active regions can be reaccelerated along with ambient plasma by a fast shock wave to produce impulsive abundances with reduced variations.

7) Compared with abundances in the slow solar wind (Bochsler 2009) the largest statistically important discrepancy is C/O = 0.68±0.07 in the solar wind and C/O = 0.42±0.01 in SEPs. This difference, and differences in the abundances of P and S, can be explained by photospheric temperature differences that make P and S neutral atoms in sunspots beneath SEP sources, but ions in the solar wind. This difference affects their FIP-dependent transport from photosphere to corona.

8) Some regions of the shock waves in many gradual SEP events also sample recently-formed high coronal loops where the slowly-evolving He abundance has attained as little as half of its full value.

9) CME-driven shock waves are able to accelerate ions to energies high enough for these new SEPs to easily escape closed, but weak, magnetic loops in the high corona with footpoints in cool sunspots. The solar wind must exit the corona on more open field lines that have footpoints with higher photospheric temperatures.

10) Maps of Si/S abundance in the corona show enhancements near active regions that are the origin of SEPs, but Si/S enhancements cannot show the origin of the slow solar wind since both Si and S are low-FIP ions in the solar wind.

Abundances of elements and isotopes tell a rich story of the physical processes that characterize SEPs.

The author thanks Ed Cliver and Steve Kahler for helpful discussions and comments on this manuscript.

## References

Arnaud, M., Rothenflug, R., An updated evaluation of recombination and ionization rates, *Astron. Astrophys. Suppl.* **60**, 425 (1985)

Asplund, M., Grevesse, N., Sauval, A.J., Scott, P.: The chemical composition of the sun. *Annu. Rev. Astron. Astrophys.* **47**, 481 (2009)

Bertch, D. L., Fichtel, C. E., Reames, D. V., Relative abundance of iron-group nuclei in solar cosmic rays, *Astrophys. J. Lett.* **157**, L53 (1969)

Bochsler, P., Solar abundances of oxygen and neon derived from solar wind observations, *Astron. Astrophys.* **471** 315 (2007)

Bochsler, P., Composition of matter in the heliosphere, *Proc. IAU Sympos.* **257**, 17 (2009) doi:10.1017/S1743921309029044.

Breneman, H.H., Stone, E.C., Solar coronal and photospheric abundances from solar energetic particle measurements, *Astrophys. J. Lett.* **299**, L57 (1985)

Brooks, D.H., Ugarte-Urra, I., Warren, H.P., Full-Sun observations for identifying the source of the slow solar wind, *Nature Comms.* **6**, 5947 (2016)

Bućik, R., Innes, D.E., Mall, U., Korth, A., Mason, G.M., Gómez-Herrero, R., Multi-spacecraft observations of recurrent  $^3\text{He}$ -rich solar energetic particles, *Astrophys. J.* **786**, 71 (2014)

Bućik, R., Innes, D.E., Chen, N.H., Mason, G.M., Gómez-Herrero, R., Wiedenbeck, M.E., Long-lived energetic particle source regions on the Sun, *J. Phys. Conf. Ser.* **642**, 012002 (2015)

Caffau, E., Ludwig, H.-G., Steffen, M., Freytag, B., Bonofacio, P., Solar chemical abundances determined with a CO5BOLD 3D model atmosphere, *Solar Phys.* **268**, 255. (2011) doi:10.1007/s11207-010-9541-4

Carrington, R.C. Description of a singular appearance seen in the Sun on September, 1859, *Mon. Not. Roy. Astron. Soc.* **20**, 13 (1860)

Chen N.H., Bućik R., Innes D.E., Mason G.M., Case studies of multi-day  $^3\text{He}$ -rich solar energetic particle periods, *Astron. Astrophys.* **580**, 16 (2015) doi: 10.1051/0004-6361/201525618

Cliver, E.W., Flare vs. shock acceleration of high-energy protons in solar energetic particle events, *Astrophys. J.* **832** 128 (2016)

Cliver, E.W., Ling, A.G., Electrons and protons in solar energetic particle events, *Astrophys. J.* **658**, 1349 (2007)

Cliver, E.W., Kahler, S.W., and Reames, D.V., Coronal shocks and solar energetic proton events, *Astrophys. J.* **605**, 902 (2004)

Cohen, C.M.S., Mason, G.M., Mewaldt, R.A., Characteristics of solar energetic ions as a function of longitude, *Astrophys. J.* **843** 132 (2017)

Cohen, C.M.S., Mason, G.M., Mewaldt, R.A., Wiedenbeck, M.E., The longitudinal dependence of heavy-ion composition in the 2013 April 11 solar energetic particle event, *Astrophys. J.* **793** 35 (2014)

Collier, M.R., Hamilton, D.C., Gloeckler, G., Bochsler, P., Sheldon, R.B., Neon-20, oxygen-16, and helium-4 densities, temperatures, and suprathermal tails in the solar wind determined with WIND/MASS, *Geophys. Res. Lett.*, **23**, 1191 (1996)

Cook, W.R., Stone, E.C., Vogt, R.E., Elemental composition of solar energetic particles, *Astrophys. J.* **279**, 827 (1984)

Desai, M.I., Giacalone, J., Large gradual solar energetic particle events, *Living Reviews of Solar Physics*, doi: 10.1007/s41116-016-0002-5 (2016)

Desai, M.I., Mason, G.M., Dwyer, J.R., Mazur, J.E., Gold, R.E., Krimigis, S.M., Smith, C.W., Skoug, R.M., Evidence for a Suprathermal Seed Population of Heavy Ions Accelerated by Interplanetary Shocks near 1 AU, *Astrophys. J.*, **588**, 1149 (2003)

DiFabio, R., Guo, Z., Möbius, E., Klecker, B., Kucharek, H., Mason, G.M., Popecki, M., Energy-dependent charge states and their connection with ion abundances in impulsive solar energetic particle events, *Astrophys. J.* **687**, 623. (2008)

Doschek, G. A., Warren, H. P., The mysterious case of the solar argon abundance near sunspots in flares, *Astrophys. J.* **825**, 36 (2016)

Doschek, G. A., Warren, H. P., Sunspots, starspots, and elemental abundances, *Astrophys. J.* **844**, 52 (2017)

Drake, J.F., Cassak, P.A., Shay, M.A., Swisdak, M., Quataert, E., A magnetic reconnection mechanism for ion acceleration and abundance enhancements in impulsive flares, *Astrophys. J. Lett.* **700**, L16 (2009)

Evenson, P., Meyer, P., Pyle, K.R., Protons from the decay of solar flare neutrons, *Astrophys. J.* **274**, 875 (1983)

Evenson, P., Kroeger, R., Meyer, P., Reames, D., Solar neutron decay proton observations in cycle 21, *Astrophys. J. Suppl.* **73** 273 (1990)

Fichtel, C.E., Guss, D.E., Heavy nuclei in solar cosmic rays, *Phys. Rev. Lett.* **6**, 495 (1961)

Fisk, L.A.,  $^3\text{He}$ -rich flares - a possible explanation, *Astrophys. J.* **224**, 1048 (1978)

Forbush, S.E.: Three unusual cosmic ray increases possibly due to charged particles from the Sun. *Phys. Rev.* **70**, 771 (1946)

Gloeckler, G., Geiss, J., Measurement of the abundance of Helium-3 in the Sun and in the local interstellar cloud with SWICS on ULYSSES, *Space Sci. Rev.* **84** 275 (1998)

Gopalswamy, N., Xie, H., Yashiro, S., Akiyama, S., Mäkelä, P., Usoskin, I. G., Properties of Ground level enhancement events and the associated solar eruptions during solar cycle 23, *Space Sci. Rev.* **171**, 23 (2012)

Gosling, J.T.: The solar flare myth. *J. Geophys. Res.* **98**, 18937 (1993)

Heber, V.S., Burnett, D.S., Duprat, J., Guan, Y., Jurewicz, A.J.G., Marty, B., McKeegan, K.D., Carbon, nitrogen, and oxygen abundances in the bulk solar wind and calibration of absolute abundances, 44<sup>th</sup> Lunar and Planet. Sci. Conf., LPI **44** 2540 (2013).

Hsieh, K.C., Simpson, J.A., The relative abundances and energy spectra of 3He and 4He from solar flares, *Astrophys., J. Lett.* **162**, L191 (1970)

Kahler, S.W., Solar flares and coronal mass ejections, *Annu. Rev. Astron. Astrophys.* **30**, 113 (1992).

Kahler, S.W., Injection profiles of solar energetic particles as functions of coronal mass ejection heights, *Astrophys. J.*, **428**, 837 (1994)

Kahler, S.W., The correlation between solar energetic particle peak intensities and speeds of coronal mass ejections: Effects of ambient particle intensities and energy spectra, *J. Geophys. Res.* **106**, 20947 (2001)

Kahler, S.W., Reames, D.V., Solar energetic particle production by coronal mass ejection-driven shocks in solar fast-wind regions, *Astrophys. J.* **584**, 1063 (2003)

Kahler, S. W., Kazachenko, M., Lynch, B.J., Welsch, B.T., Flare magnetic reconnection fluxes as possible signatures of flare contributions to gradual SEP events, *J. Phys. Conf. Series*, In preparation (2017)

Kahler, S.W., Reames, D.V., Sheeley, N.R., Jr., Coronal mass ejections associated with impulsive solar energetic particle events, *Astrophys. J.*, **562**, 558 (2001)

Kahler, S.W., Tylka, A.J., Reames, D.V., A comparison of elemental abundance ratios in sep events in fast and slow solar wind regions, *Astrophys. J.* **701**, 561 (2009).

Kahler, S.W., Sheeley, N.R., Jr., Howard, R.A., Koomen, M.J., Michels, D.J., McGuire, R.E., von Rosenvinge, T.T., Reames, D.V., Associations between coronal mass ejections and solar energetic proton events, *J. Geophys. Res.* **89**, 9683 (1984)

Kasper, J.C., Stevens, M.L., Lazarus, A.J., Steinberg, J.T., Ogilvie, K. W., Solar wind helium abundance as a function of speed and heliographic latitude: variation through a solar cycle, *Astrophys. J.* **660**, 901 (2007)

Kazachenko, M.D., Lynch, B.J., Welsch, B.T., Sun, X., A database of flare ribbon properties from solar dynamics observatory I: Reconnection flux, arXiv:1704.05097.

Klecker, B., Current understanding of SEP acceleration and propagation, *J. Phys.: CS-409*, 012015 (2013)

Kozlovsky, B., Murphy, R.J., Ramaty, R., Nuclear deexcitation gamma-ray lines from accelerated particle interactions, *Astrophys. J. Suppl.* **141** 523 (2002)

Laming, J.M., A unified picture of the first ionization potential and inverse first ionization potential effects, *Astrophys. J.* **614**, 1063 (2004)

Laming, J.M., Non-WKB models of the first ionization potential effect: implications for solar coronal heating and the coronal helium and neon abundances, *Astrophys. J.* **695**, 954 (2009)

Laming, J.M., The FIP and inverse FIP effects in solar and stellar coronae, *Living Reviews in Solar Physics*, **12**, 2, doi: [10.1007/lrsp-2015-2](https://doi.org/10.1007/lrsp-2015-2) (2015)

Lee, M.A., Coupled hydromagnetic wave excitation and ion acceleration at interplanetary traveling shocks, *J. Geophys. Res.*, **88**, 6109. (1983)

Lee, M.A., Coupled hydromagnetic wave excitation and ion acceleration at an evolving coronal/interplanetary shock, *Astrophys. J. Suppl.*, **158**, 38 (2005)

Lee, M.A., Mewaldt, R.A., Giacalone, J., Shock acceleration of ions in the heliosphere, *Space Sci. Rev.* **173**, 247 (2012)

Leske, R.A., Cummings, J.R., Mewaldt, R.A., Stone, E.C., and von Rosenvinge, T.T., Measurements of the ionic charge states of solar energetic particles using the geomagnetic field, *Astrophys. J.* **452**, L149 (1995)

Lin, R. P., Non-relativistic solar electrons, *Space Sci. Rev.* **16**, 189 (1974)

Liu, S., Petrosian, V., Mason, G.M.: Stochastic acceleration of <sup>3</sup>He and <sup>4</sup>He in solar flares by parallel-propagating plasma waves: general results. *Astrophys. J.* **636**, 462 (2006)

Lodders, K., Palme, H., Gail, H.-P., Abundances of the elements in the solar system, In: Trümper, J.E. (ed.) *Landolt-Börnstein, New Series VI/4B*, Springer, Berlin. Chap. **4.4**, 560 (2009).

Luhn, A., Klecker, B., Hovestadt, D., Gloeckler, G., Ipvavich, F. M., Scholer, M., Fan, C. Y., Fisk, L. A., Ionic charge states of N, Ne, Mg, Si and S in solar energetic particle events, *Adv. Space Res.* **4**, 161 (1984)

Luhn, A., Klecker, B., Hovestadt, D., Möbius, E., The mean ionic charge of silicon in He-3-rich solar flares, *Astrophys. J.* **317**, 951 (1987).

Mandzhavidze, N., Ramaty, R., Kozlovsky, B., Determination of the abundances of subcoronal <sup>4</sup>He and of solar flare-accelerated <sup>3</sup>He and <sup>4</sup>He from gamma-ray spectroscopy, *Astrophys. J.* **518**, 918 (1999)

Mason, G.M.: <sup>3</sup>He-rich solar energetic particle events. *Space Sci. Rev.* **130**, 231 (2007)

Mason, G.M., Gloeckler, G., Hovestadt, D., Temporal variations of nucleonic abundances in solar flare energetic particle events. II - Evidence for large-scale shock acceleration, *Astrophys. J.* **280**, 902 (1984)

Mason, G.M., Mazur, J.E., Dwyer, J.R., <sup>3</sup>He enhancements in large solar energetic particle events, *Astrophys. J. Lett.* **525**, L133 (1999)

Mason, G.M., Mazur, J.E., Dwyer, J.R.: A new heavy ion abundance enrichment pattern in <sup>3</sup>He-rich solar particle events. *Astrophys. J. Lett.* **565**, L51 (2002)

Mason, G.M., Mazur, J.E., Dwyer, J.R., Jokipii, J.R., Gold, R.E., Krimigis, S.M., Abundances of heavy and ultraheavy ions in <sup>3</sup>He-rich solar flares, *Astrophys. J.* **606**, 555 (2004).

Mason, G.M., Nitta, N.V., Wiedenbeck, M.E., Innes, D.E.: Evidence for a common acceleration mechanism for enrichments of <sup>3</sup>He and heavy ions in impulsive SEP events. *Astrophys. J.* **823**, 138 (2016)

Mason, G.M., Reames, D. V., Klecker, B., Hovestadt, D., von Rosenvinge, T.T., The heavy-ion compositional signature in He-3-rich solar particle events, *Astrophys. J.* **303**, 849 (1986)

Mazzotta, P., Mazzitelli, G., Colafrancesco, S., Vittorio, N., Ionization balance for optically thin plasmas: Rate coefficients for all atoms and ions of the elements H to Ni, *Astron. Astrophys. Suppl.* **133**, 403 (1998).

McGuire, R.E., von Rosenvinge, T.T., McDonald, F.B., A survey of solar cosmic ray composition, *Proc. 16<sup>th</sup> Int. Cosmic Ray Conf., Tokyo* **5**, 61 (1979)

Mewaldt, R.A., Cohen, C.M.S., Leske, R.A., Christian, E.R., Cummings, A.C., Stone, E.C., von Rosenvinge, T.T. and Wiedenbeck, M. E., Fractionation of solar energetic particles and solar wind according to first ionization potential, *Advan. Space Res.*, **30**, 79 (2002).

Mewaldt, R.A.,Looper, M.D., Cohen, C.M.S., Haggerty, D.K., Labrador, A.W., Leske, R.A., Mason, G.M., Mazur, J.E., von Rosenvinge, T.T., Energy spectra, composition, other properties of ground-level events during solar cycle 23, *Space Sci. Rev.* **171**, 97 (2012)

Meyer, J.P., The baseline composition of solar energetic particles, *Astrophys. J. Suppl.* **57**, 151 (1985)

Murphy, R.J., Ramaty, R., Kozlovsky, B., Reames, D.V., Solar abundances from gamma-ray spectroscopy: Comparisons with energetic particle, photospheric, and coronal abundances, *Astrophys. J.* **371**, 793 (1991)

Murphy, R.J., Kozlovsky, B., Share, G.H.; Evidence for enhanced  $^3\text{He}$  in flare-accelerated particles based on new calculations of the gamma-ray line spectrum, *Astrophys.J.* **833**, 166 (2016)

Ng, C.K., Reames, D.V., Shock acceleration of solar energetic protons: the first 10 minutes, *Astrophys. J. Lett.* **686**, L123 (2008)

Ng, C.K., Reames, D.V., Tylka, A.J., Modeling shock-accelerated solar energetic particles coupled to interplanetary Alfvén waves, *Astrophys. J.* **591**, 461 (2003)

Parker, E.N.: Nanoflares and the solar X-ray corona. *Astrophys. J.* **330**, 474 (1988)

Post, D.E., Jensen, R.V., Tarter, C.B., Grasberger, W.H., Lokke, W.A., Steady-state radiative cooling rates for low-density, high temperature plasmas, *At. Data Nucl. Data Tables* **20**, 397 (1977)

Rakowsky, C.E., Laming, J. M., On the Origin of the slow speed solar wind: helium abundance variations, *Astrophys. J.* **754**, 65 (2012)

Ramaty, R., Murphy, R. J., Nuclear processes and accelerated particles in solar flares, *Space Sci. Rev.* **45**, 213 (1987)

Raouafi, N.E., Patsourakos, S., Pariat, E., Young, P.R., Sterling, A.C., Savcheva, A., Shimojo, M., Moreno-Insertis, F., DeVore, C.R., Archontis, V., et al., Solar coronal jets: observations, theory, and modeling, *Space Sci. Rev.* **201** 1 (2016) doi: [10.1007/s11214-016-0260-5](https://doi.org/10.1007/s11214-016-0260-5) (arXiv:1607.02108)

Reames, D.V., Bimodal abundances in the energetic particles of solar and interplanetary origin, *Astrophys. J. Lett.* **330**, L71 (1988)

Reames, D.V., Coronal Abundances determined from energetic particles, *Adv. Space Res.* **15** (7), 41 (1995)

Reames, D. V., Particle acceleration at the sun and in the heliosphere, *Space Sci. Rev.* **90**, 413 (1999)

Reames, D.V., Abundances of trans-iron elements in solar energetic particle events, *Astrophys. J. Lett.* **540**, L111 (2000)

Reames, D.V., Magnetic topology of impulsive and gradual solar energetic particle events, *Astrophys. J. Lett.* **571**, L63 (2002)

Reames, D. V., Solar release times of energetic particles in ground-level events, *Astrophys. J.* **693**, 812 (2009a)

Reames, D. V., Solar energetic-particle release times in historic ground-level events, *Astrophys. J.* **706**, 844 (2009b)

Reames, D.V., The two sources of solar energetic particles, *Space Sci. Rev.* **175**, 53 (2013)

Reames, D.V., Element abundances in solar energetic particles and the solar corona, *Solar Phys.*, **289**, 977 (2014)

Reames, D.V., What are the sources of solar energetic particles? Element abundances and source plasma temperatures, *Space Sci. Rev.* **194** 303 (2015)

Reames, D.V., Temperature of the source plasma in gradual solar energetic particle events, *Solar Phys.*, **291** 911 (2016a) doi: [10.1007/s11207-016-0854-9](https://doi.org/10.1007/s11207-016-0854-9), arXiv: 1509.08948

Reames, D.V., The origin of element abundance variations in solar energetic particles, *Solar Phys.*, **291** 2099 (2016b) doi: [10.1007/s11207-016-0942-x](https://doi.org/10.1007/s11207-016-0942-x), arXiv: 1603.06233

Reames, D.V., Element abundances and source plasma temperatures of solar energetic particles, *J. Phys. Conf. Series* **767** 012023 (2016c) doi: [10.1088/1742-6596/767/1/012023](https://doi.org/10.1088/1742-6596/767/1/012023) (arXiv: [1612.00030](https://arxiv.org/abs/1612.00030))

Reames D.V., *Solar Energetic Particles*, Springer, Berlin, (2017a) ISBN 978-3-319-50870-2, DOI 10.1007/978-3-319-50871-9.

Reames, D.V., Spatial distribution of element abundances and ionization states in solar energetic-particle events, *Solar Phys.* **292** 133 (2017b), doi: [10.1007/s11207-017-1138-8](https://doi.org/10.1007/s11207-017-1138-8) (arXiv: [1705.07471](https://arxiv.org/abs/1705.07471))

Reames, D.V., The abundance of helium in the source plasma of solar energetic particles, *Solar Phys.* in press (2017c) (arXiv: [1708.05034](https://arxiv.org/abs/1708.05034))

Reames, D.V., Ng, C.K., Heavy-element abundances in solar energetic particle events, *Astrophys. J.* **610**, 510 (2004)

Reames, D.V., Stone, R.G., The identification of solar  $^3\text{He}$ -rich events and the study of particle acceleration at the sun, *Astrophys. J.* **308**, 902 (1986)

Reames, D.V., Cliver, E.W., Kahler, S.W., Abundance enhancements in impulsive solar energetic-particle events with associated coronal mass ejections, *Solar Phys.* **289**, 3817, (2014a) doi: [10.1007/s11207-014-0547-1](https://doi.org/10.1007/s11207-014-0547-1)

Reames, D.V., Cliver, E.W., Kahler, S.W., Variations in abundance enhancements in impulsive solar energetic-particle events and related CMEs and flares, *Solar Phys.* **289**, 4675 (2014b) doi: [10.1007/s11207-014-0589-4](https://doi.org/10.1007/s11207-014-0589-4)

Reames, D.V., Cliver, E.W., Kahler, S.W.: Temperature of the source plasma for impulsive solar energetic particles. *Sol. Phys.* **290**, 1761 (2015). doi:10.1007/s11207-015-0711-2. (arXiv: 1505.02741)

Reames, D.V., Meyer, J.P., von Rosenvinge, T.T., Energetic-particle abundances in impulsive solar flare events, *Astrophys. J. Suppl.* **90**, 649 (1994)

Reames, D.V., Ng, C.K., Berdichevsky, D., Angular distributions of solar energetic particles, *Astrophys. J.* **550**, 1064 (2001)

Reames, D.V., Ng, C.K., Tylka, A.J., Initial time dependence of abundances in solar particle events, *Astrophys. J. Lett.* **531** L83 (2000)

Reames, D.V., von Rosenvinge, T.T., Lin, R.P., Solar  $^3\text{He}$ -rich events and nonrelativistic electron events - A new association, *Astrophys. J.* **292**, 716 (1985)

Roth, I., Temerin, M., Enrichment of  $^3\text{He}$  and Heavy Ions in Impulsive Solar Flares, *Astrophys. J.* **477**, 940 (1997)

Rouillard, A.C., Odstrčil, D., Sheeley, N.R. Jr., Tylka, A.J., Vourlidas, A., Mason, G., Wu, C.-C., Savani, N.P., Wood, B.E., Ng, C.K., et al., Interpreting the properties of solar energetic particle events by using combined imaging and modeling of interplanetary shocks, *Astrophys. J.* **735**, 7 (2011)

Rouillard, A.P., Plotnikov, I., Pinto, R.F., Tirole, M., Lavarra, M., Zucca, P., Vainio, R., Tylka, A.J., Vourlidas, A., De Rosa, M. L., et al., Deriving the properties of coronal pressure fronts in 3D: application to the 2012 May 17 ground level enhancement, *Astrophys. J.* **833** 45 (2016)

Rouillard, A., Sheeley, N.R. Jr., Tylka, A., Vourlidas, A., Ng, C.K., Rakowski, C., Cohen, C.M.S., Mewaldt, R.A., Mason, G.M., Reames, D., et al., The longitudinal properties of a solar energetic particle event investigated using modern solar imaging, *Astrophys. J.* **752**, 44 (2012)

Schmelz, J. T., Reames, D. V., von Steiger, R., Basu, S., Composition of the solar corona, solar wind, and solar energetic particles, *Astrophys. J.* **755** 33 (2012)

Serlemitsos, A.T., Balasubrahmanyam, V.K., Solar particle events with anomalously large relative abundance of  $^3\text{He}$ , *Astrophys. J.* **198**, 195, (1975)

Shimojo, M., Shibata, K., Physical parameters of solar X-ray jets, *Astrophys. J.* 542, 1100 (2000)

Teegarden, B.J., von Rosenvinge, T.T., McDonald, F.B., Satellite measurements of the charge composition of solar cosmic rays in the  $6 \leq Z \leq 26$  interval, *Astrophys. J.* **180**, (1973)

Temerin, M., Roth, I., The production of  $^3\text{He}$  and heavy ion enrichment in  $^3\text{He}$ -rich flares by electromagnetic hydrogen cyclotron waves, *Astrophys. J. Lett.* **391**, L105 (1992).

Tylka, A.J., Boberg, P.R., Adams, J.H., Jr., Beahm, L.P., Dietrich, W.F., Kleis, T., The mean ionic charge state of solar energetic Fe ions above 200 MeV per nucleon, *Astrophys. J.* **444**, L109 (1995)

Tylka, A.J., Cohen, C.M.S., Dietrich, W.F., Lee, M.A., MacLennan, C.G., Mewaldt, R.A., Ng, C.K., Reames, D.V., Shock geometry, seed populations, and the origin of variable elemental composition at high energies in large gradual solar particle events, *Astrophys. J.* **625**, 474 (2005)

Tylka, A.J., Lee, M.A., Spectral and compositional characteristics of gradual and impulsive solar energetic particle events, *Astrophys. J.* **646**, 1319 (2006)

Vrsnak, B., Cliver, E.W., Origin of coronal shock waves, Invited review, *Solar Phys.* **253** 215 (2008).

Webber, W.R., Solar and galactic cosmic ray abundances - A comparison and some comments. *Proc. 14<sup>th</sup> Int. Cos. Ray Conf., Munich*, **5**, 1597 (1975)

Zank, G.P., Li, G., Verkhoglyadova, O., Particle Acceleration at Interplanetary Shocks, *Space Sci. Rev.* **130**, 255 (2007)

Zank, G.P., Rice, W.K.M., Wu, C.C., Particle acceleration and coronal mass ejection driven shocks: A theoretical model, *J. Geophys. Res.*, 105, 25079 (2000)